A More Conservative Form of Governing Equations in RELAP5

A Thesis

Presented in Partial Fulfillment of the Requirements for the

Degree of Master of Science

with a

Major in Mechanical Engineering

in the

College of Graduate Studies

University of Idaho

by

Zheng Fu

November 2014

Major Professor: Fatih Aydogan

Authorization to Submit Thesis

This thesis of Zheng Fu, submitted for the degree of Master of Science with a Major in Mechanical Engineering and titled "A More Conservative Form of Governing Equations in RELAP5," has been reviewed in final form. Permission, as indicated by the signatures and dates below, is now granted to submit final copies to the College of Graduate Studies for approval.

Major Professor: _____ Date: _____
Fatih Aydogan, Ph.D.

Committee Members: _____ Date: _____
Ray A. Berry, Ph.D.

_____ Date: _____
Richard J. Wagner, M.S.

Department Administrator: _____ Date: _____
John Crepeau, Ph.D.

Discipline's College Dean: _____ Date: _____
Larry Stauffer, Ph.D.

Final Approval and Acceptance

Dean of the College Of Graduate Studies: _____Date: _____
Jie Chen, Ph.D.

Abstract

RELAP5 is based on a two-fluid, non-equilibrium, non-homogeneous, hydrodynamic model for the transient simulation of the two-phase flow system behavior. In current versions of RELAP5, the “non-conservative” numerical approximation form is used. For discretization of the non-conservative form, the truncation errors introduced in the linearization process can produce mass and energy errors for some classes of transients during time advancements, either resulting in (a) automatic reduction of time steps used in the advancement of the equations and increased run times or (b) the growth of unacceptably large errors in the transient results. To eliminate these difficulties, a more conservative numerical approach has been introduced and implemented into RELAP5/SCDAP. This article demonstrates the theory of both the non-conservative and the developed conservative numerical approach. It also introduces the solution strategy of the more conservative approach and presents the code-to-code comparison between the non-conservative and more conservative approaches. RELAP5/SCDAP mode 4.0 versions are utilized for the code-to-code comparisons. These comparisons results prove that mass error is significantly reduced by implementing the more conservative numerical approximation.

KEYWORDS: RELAP5, conservative numerical approximation, semi-implicit solution strategy

Acknowledgements

I am using this opportunity to express my gratitude to everyone who supported me throughout the course of this project. I am thankful for their inspiring guidance, invaluably constructive criticism, and friendly advice during the project work. I am sincerely grateful to them for sharing their truthful and illuminating views on a number of issues related to the project.

I express my warm thanks to Mr. Wagner for his support and guidance at Innovative System Software and Dr. Aydogan at the Center for Advanced Energy Studies.

I would also like to thank my project external guide Mr. Allison from Innovative Systems Software and all the people who provided me with the facilities being required and conductive conditions for this project.

Dedication

I would like to thank my parents and my step-father for their support during my studies at the University of Idaho.

Table of Contents

List of Figures

List of Tables

List of Abbreviations

A_f, A	flow area (m^2)
$DISS_g$, $DISS_f$	phasic energy dissipation terms (W/m^3)
FWF, FWG	wall drag coefficients (liquid, vapor/gas) (s^{-1})
gammaw	mass transfer rate per unit volume at the vapor/liquid interface in the boundary layer near the wall for vapor generation (kg/m^3s)
H	volumetric heat transfer coefficient (W/Km^3)
h	heat transfer coefficient (W/m^2K); specific enthalpy (J/kg)
h^o_g ,h^o_f	phasic specific enthalpies associated with bulk interface mass transfer
$h`_g$ ,$h`_f$	phasic specific enthalpies associated with wall interface mass transfer
htrnrn	heat flux (W/m^2)
htvat	volume-averaged temperature in the heat structure (K)
L	length (m)
P	pressure (Pa)
Ps	partial pressure (Pa)
Q	volumetric heat addition rate (W/m^3)
Qwg, Qwf	wall heat transfer
Qig, Qif	interphase heat transfer
Qgf	interface (direct) heating term
q	heat flux (W/m^2)

S	surface
T	temperature (K)
T^s	saturation temperature function corresponding to total pressure
$T^s(P_s)$	saturation temperature function corresponding to partial pressure
t	time (s)
Uf	liquid internal energy (J/kg)
Ug	vapor internal energy (J/kg)
u	specific internal energy (J/kg)
V	volume (m^3)
v	mixture velocity (m/s), phasic velocity (m/s)
vapgen	vapor generation rate (kg/m^3s)
voidg	vapor void fraction
X	non-condensable quality
Xs	statics quality

List of Symbols

α	void fraction
ρ	density (kg/m^3)
Γ	volumetric mass exchange rate (kg/m^3s)
Γ_{ig}	interphase mass exchange rate (kg/m^3s)
Γ_e	interphase energy exchange rate (W/m^3)
Δ	difference, increment

List of Superscripts

B	bulk liquid
m	old time value
m+1	new time value
s	saturation property
o	initial value

List of Subscripts

w	wall, boiling at wall
c	condensation at wall
i	volume index
i+1	next iteration value
n	non-condensable gases
g	vapor phase
f	liquid phase
ig	interphase
o	reference value
sp	saturation function corresponding to partial pressure
sT	saturation function corresponding to total pressure
wgg, gg	coefficient to vapor/gas, with the vapor/gas temperature as the reference temperature
wgspt, gT	coefficient to vapor/gas, with the saturation temperature based on the total pressure as the reference temperature
wgspp, gs	coefficient to vapor/gas, with the saturation temperature based on the vapor partial pressure as the reference temperature
wff, ff	coefficient to liquid, with the vapor/gas temperature as the reference temperature
wfspt, fT	coefficient to liquid, with the saturation temperature based on the total pressure as the reference temperature

wfspp, fs	coefficient to liquid, with the saturation temperature based on the vapor partial pressure as the reference temperature
ρg	function of vapor density
ρf	function of liquid density
Tg	function of vapor temperature
Tf	function of liquid temperature
T	to junction (in summation notation)
F	from junction (in summation notation)
j	junction quantity (in summation notation)

Chapter 1: Introduction

RELAP5 (Reactor Excursion and Leak Analysis Program) is one of the commonly used nuclear safety codes for nuclear safety licensing and analyzing nuclear power plant systems. It includes six governing equations for two fields (liquid and vapor). Conservative and non-conservative methods are two numerical approaches used for the solution of governing equations. However, a feature of the more conservative form of approximation is better preservation of energy and mass in a system. Examples of the conservative and non-conservative numerical approximations are shown in Figure 1.

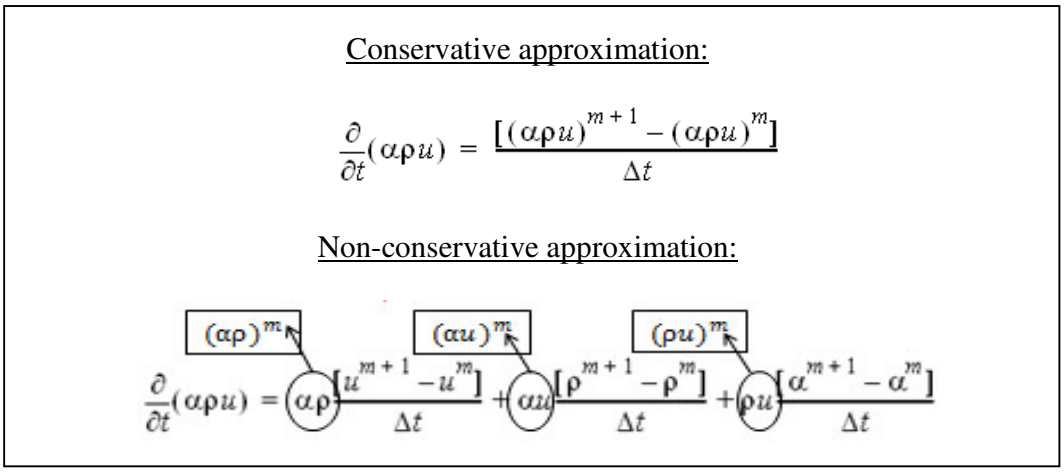

Figure 1: Examples of Conservative and Non-conservative Numerical Approximations

The superscripts indicate time levels, with 'm+1' meaning new time value and m meaning old time value. Clearly, non-conservative approximation uses old time values for the coefficients in front of derivative terms. Therefore, it does not express an exact conservation principle in finite volume form.

The current RELAP5 numerical scheme has two steps to evaluate basic conservation equations. The first evaluation uses non-conservative numerical approximation and the

truncation errors in the linearization procedure of non-conservative numerical approximation may produce mass and energy errors during the advancement. The second step of semi-implicit scheme is to use the intermediate time variables, which are from non-conservative forms (expanded forms), to re-compute vapor/liquid internal energies and non-condensable fraction in the conservative forms (unexpanded forms) of governing equations. Because of utilizing the conservative forms, current RELAP5 is considered as a 'conservative' code. However, it is not fully conservative due to the fact that the final pressure value is obtained by using non-conservative forms. Moreover, void fraction and phasic densities are all a function of the pressure.

Therefore, when the transfers of masses and energies in the system are summed at the entrance and exit boundary conditions, the summed values can be different from summation of mass or energy of each volume in the system (NSAD, 2001). Switching to the consistent conservative form of numerical approach reduces the loss or gain of mass and energy. This work focuses only on time derivative terms in mass and energy governing equations. The conservative forms of the momentum equation and the space derivative terms in mass/ energy equations are not part of the study.

Codes with the fully conservative forms of governing equations have an advantage over others (Mahaffy, 1993) and the current RELAP5 is not a fully conservative code. Therefore, this work focuses on developing, implementing, and solving a set of more conservative mass and energy equations in RELAP5. The paper presents five conservative approximations of mass and energy balance equations alone with sixteen constitutive equations. Then, a solution strategy for the more conservative form of governing equations is introduced. The new solution method constructs one matrix for each system with the balance

equations and constitutive equations. It solves the matrix to obtain the changes in all new time variables simultaneously. The system matrix is composed of two sub-matrices including volume balance equations (mass and energy) and junction conservation equations (momentum). Since the conservative numerical approximation is applied only for mass and energy governing equations, the article gives only the coefficients used to build volume mass-energy sub-matrix with conservative mass-energy balance equations and their closure equations. Moreover, the preliminary tests show the comparison results between the fully conservative and non-conservative approaches in RELAP5 (G. A. Roth, F. Aydogan, 2014a, 2014b). The improved code is implemented into RELAP5/SCDAP mod 4.0 version. The code verification was done by using the US-NRC's Regulatory Guide 1.203 (Rg 1.203, 2005)

Chapter 2: Mass/Energy Balance Equations and Closure Equations

The RELAP5 thermal-hydraulic model solves six governing equations including liquid/vapor mass continuity, liquid/vapor energy conservation, and liquid/vapor momentum conservation and two additional equations for non-condensable mass conservation and conservation of solute (i.e., boron). In order to solve the non-linearized mass and energy partial differential equations, numerical approximations are used to linearize mass and energy differential equations. Before introducing numerical solution in next section, the basic mass and energy differential equations in RELAP5 are demonstrated starting from equations 1 through 5 (NSAD, 2001). These partial differential equations are the same for both the non-conservative and conservative numerical approximations. Equations 1 through 5 demonstrate mass and energy conservation equations. The procedures for the momentum equations are the same as in RELAP5 and are not included in the following derivations.

Conservation of Mass of Non-condensable Gases

$$\frac{\partial}{\partial t}\left(\alpha_g \rho_g X_n\right) = -\nabla \cdot \alpha_g \rho_g X_n \bar{v}_g \tag{1}$$

Conservation of Vapor Mass

$$\frac{\partial}{\partial t}\left(\alpha_g \rho_g\right) = -\nabla \cdot \alpha_g \rho_g \bar{v}_g + \Gamma_{ig} + \Gamma_w + \Gamma_c \tag{2}$$

Conservation of Liquid Mass

$$\frac{\partial}{\partial t}\left(\alpha_f \rho_f\right) = -\nabla \cdot \alpha_f \rho_f \bar{v}_f - \Gamma_{ig} - \Gamma_w - \Gamma_c \tag{3}$$

The conservation mass equations are from the one-dimensional phasic mass equations (Ransom, V.H., 1989). In equations 1 through 3, the terms on the left hand sides are the time rate of change of the mass. The first terms on the right hand sides are the change in mass due to the mass entering of leaving the control volume. The Γ_{ig} is the bulk interface volumetric mass exchange rate between liquid and vapor. Γ_w is the boiling mass transfer in the boundary layers near the walls and Γ_c is the condensing mass transfer in the boundary layers near walls (Roth, G. A., Aydogan, F., 2014a, 2014b).

Balance of Vapor Internal Energy

$$\frac{\partial}{\partial t}\left(\alpha_g \rho_g u_g\right) = -\nabla \cdot \alpha_g \rho_g u_g \bar{v}_g - P\frac{\partial \alpha_g}{\partial t} - P\left(\nabla \cdot \alpha_g \bar{v}_g\right) + \Gamma_{ig} h_g^{\circ} + \Gamma_w h_{wg}^{`} + \Gamma_c h_{cg}^{`} + Q_{wg} + Q_{ig} - Q_{gf} + \alpha_g \rho_g FWG v_g^2 \quad (4)$$

Balance of Liquid Internal Energy

$$\frac{\partial}{\partial t}\left(\alpha_f \rho_f u_f\right) = -\nabla \cdot \alpha_f \rho_f u_f \bar{v}_f - P\frac{\partial \alpha_f}{\partial t} - P\left(\nabla \cdot \alpha_f \bar{v}_f\right) - \Gamma_{ig} h_f^{\circ} + \Gamma_w h_{wf}^{`} + \Gamma_c h_{cf}^{`} + Q_{wf} + Q_{if} - Q_{gf} + \alpha_f \rho_f FWF v_f^2 \quad (5)$$

The energy equations also come from the one-dimensional phasic thermal energy equations (Ransom, V.H., 1989). To obtain RELAP balance energy equations from 1D phasic thermal energy equations, the following simplifications are used:

- The Reynolds heat flux is neglected
- Covariance terms are universally neglected
- Interfacial energy storage is neglected
- Internal phasic heat transfer is neglected

In RELAP5 conservation of energy equations 4 and 5, the term on the left hand side is the time rate of change of the energy for both liquid and vapor phase. The first two terms on the right hand sides of energy equations are energy change due to mass crossing boundary by convection and energy change due to time rate of change in volume faction separately. The third term of right hand side represents power of compression working due to volumetric straining (Roth, G. A., Aydogan, F., 2014a, 2014b).

Energy exchanges due to phase change are represented with terms - $\Gamma_{ig} h_f^{\circ}$, $\Gamma_w h_{wf}^{`}$, and $\Gamma_c h_{cf}^{`}$. Q_{gf} is the sensible heat transfer rate per unit volume and it is the heat transfer at the non-condensable gas-liquid interface. It represents thermal energy exchange between the bulk fluid states themselves when non-condensable gas is present. Q_{if}/Q_{ig} is the heat transfer from interface to liquid/vapor and Q_{wf}/Q_{wg} is the heat transfer to liquid/ vapor from the wall (Roth, G. A., Aydogan, F., 2014a, 2014b).

The last terms in equations 4 and 5 represent the phasic mechanical energy dissipation terms. Notice the phasic energy dissipation terms, $DISS_f$ and $DISS_g$, are written here in terms of the product of α, ρ, v^2, and wall drag coefficients for liquid and vapor/gas (FWF/FWG). Moreover, mass transfer between phases near the wall is again split into a boiling part (Γ_w) and condensing part (Γ_c) (NSAD, 2001).

In these equations, the time derivative quantity is the same as the quantity convected in the convection term. Integrating these equations over the volume and applying the divergence theorem to the convective terms, the above conservation Equations 1-5 are transferred into integral differential form and become Equations 6-10.

Conservation of Mass of Non-condensable Gases in Integral Form

$$\int_V \frac{\partial}{\partial t}(\alpha_g \rho_g X_n) dV = -\int_S \alpha_g \rho_g X_n \bar{v}_g \cdot d\bar{S} \quad (6)$$

Conservation of Vapor Mass in Integral For

$$\int_V \frac{\partial}{\partial t}(\alpha_g \rho_g) dV = -\int_S \alpha_g \rho_g \bar{v}_g \cdot d\bar{S} + \int_V (\Gamma_{ig} + \Gamma_w + \Gamma_c) dV \quad (7)$$

Conservation of Liquid Mass in Integral Form

$$\int_V \frac{\partial}{\partial t}(\alpha_f \rho_f) dV = -\int_S \alpha_f \rho_f \bar{v}_f \cdot d\bar{S} - \int_V (\Gamma_{ig} + \Gamma_w + \Gamma_c) dV \quad (8)$$

Balance of Vapor Internal Energy in Integral Form

$$\int_V \frac{\partial}{\partial t}(\alpha_g \rho_g u_g) dV = -\int_S \alpha_g \rho_g u_g \bar{v}_g \cdot d\bar{S} - \int_V P \frac{\partial \alpha_g}{\partial t} dV - \int_S P \alpha_g \bar{v}_g \cdot d\bar{S} + \int_V (\Gamma_{ig} h_g^{\circ} + \Gamma_w h_{wg}^{`} + \Gamma_c h_{cg}^{`} + Q_{wg} + Q_{ig} - Q_{gf} + \alpha_g \rho_g FWG v_g^2) dV \quad (9)$$

Balance of Liquid Internal Energy in Integral Form

$$\int_V \frac{\partial}{\partial t}(\alpha_f \rho_f u_f) dV = -\int_S \alpha_f \rho_f u_f \bar{v}_f \cdot d\bar{S} - \int_V P \frac{\partial \alpha_f}{\partial t} dV - \int_S P \alpha_f \bar{v}_f \cdot d\bar{S} - \int_V (\Gamma_{ig} h_f^{\circ} + \Gamma_w h_{wf}^{`} + \Gamma_c h_{cf}^{`} - Q_{wf} - Q_{if} - Q_{gf} - \alpha_f \rho_f FWF v_f^2) dV \quad (10)$$

Additional algebraic equations are required to have a set of simultaneous equations that can be solved. These equations, constitutive or closure equations, are given in Equations 11-23.

Void Fraction Relationship

$$\alpha_g + \alpha_f = 1 \tag{11}$$

Thermodynamic State for Vapor Density

$$\rho_g = F_{\rho g}(P, u_g, X_n) \tag{12}$$

Thermodynamic State for Liquid Density

$$\rho_f = F_{\rho f}(P, u_f) \tag{13}$$

Thermodynamic State for Vapor Temperature

$$T_g = F_{Tg}(P, u_g, X_n) \tag{14}$$

Thermodynamic State for Liquid Temperature

$$T_f = F_{Tf}(P, u_f) \tag{15}$$

Saturation Temperature Corresponding to Partial Pressure of Water Vapor

$$T_s = F_{sp}(P_s) \tag{16}$$

Saturation Temperature Corresponding to Total Pressure

$$T_T = F_{sT}(P) \tag{17}$$

Interface Mass Transfer

$$\Gamma_{ig} = -\frac{H_{ig}[T_s - T_g] + H_{if}[T_s - T_f]}{h_g^\circ - h_f^\circ} \tag{18}$$

The interface energy is the sum of bulk interface heat transfer (Q^B_{ig} or Q^B_{if}) and energy exchange due to interface mass transfer ($h_g^\circ \Gamma_{ig}$ or $h_f^\circ \Gamma_{if}$).

$$\Gamma_e = Q_{ig}^B + h_g^\circ \Gamma_{ig} = Q_{if}^B + h_f^\circ \Gamma_{ig} = -\frac{h_f^\circ H_{ig}[T_s - T_g] + h_g^\circ H_{if}[T_s - T_f]}{h_g^\circ - h_f^\circ} \quad (19)$$

Mass Transfer at Wall Due to Flashing

$$\Gamma_w = \Gamma_{wfo} + \Gamma_{wff}\Delta T_f + \Gamma_{wfg}\Delta T_g + \Gamma_{wfspt}\Delta T_T + \Gamma_{wfspp}\Delta T_s \quad (20)$$

Mass Transfer at Wall Due to Condensation

$$\Gamma_c = \Gamma_{wgo} + \Gamma_{wgf}\Delta T_f + \Gamma_{wgg}\Delta T_g + \Gamma_{wgspt}\Delta T_T + \Gamma_{wgspp}\Delta T_s \quad (21)$$

Wall Heat Transfer to Vapor

$$Q_{wg} = Q_{wgo} + Q_{wgf}\Delta T_f + Q_{wgg}\Delta T_g + Q_{wgspt}\Delta T_T + Q_{wgspp}\Delta T_s \quad (22)$$

Wall Heat Transfer to Liquid

$$Q_{wf} = Q_{wfo} + Q_{wff}\Delta T_f + Q\Gamma_{wfg}\Delta T_g + Q_{wfspt}\Delta T_T + Q_{wfspp}\Delta T_s \quad (23)$$

This section presents mass and energy conservation equations in both differential and integral-differential forms along with thirteen thermodynamic state and transfer relations. For this study, fundamental field equations are not changed; instead, the study focuses on using a different numerical approximation approach to solve these equations. The following sections first present the current RELAP5 numerical approximation method (non-conservative form). Then, it presents the new approximation approach method (more conservative form).

Chapter 3: Conservation Equations in Non-conservative Forms

The following procedures are used in the current Relap5 thermal hydraulic model (NSAD, 2001) and are called the non-conservative form of the numerical approximation to the two-phase thermal hydraulic equations.

The time derivatives of the product terms in the partial differential (Equations 6-10) are replaced by the differentiated products to obtain Equations 24 through 28. Note that this is an exact mathematical operation. The results are:

Conservation of Mass of Non-condensable Gases

$$\int_V [\alpha_g \rho_g \frac{\partial X_n}{\partial t} + \alpha_g X_n \frac{\partial \rho_g}{\partial t} + \rho_g X_n \frac{\partial \alpha_g}{\partial t}] dV = -\int_S \alpha_g \rho_g X_n \bar{v}_g \cdot d\bar{S} \quad (24)$$

Conservation of Vapor Mass

$$\int_V [\alpha_g \frac{\partial \rho_g}{\partial t} + \rho_g \frac{\partial \alpha_g}{\partial t}] dV = -\int_S \alpha_g \rho_g \bar{v}_g \cdot d\bar{S} + \int_V (\Gamma_{ig} + \Gamma_w + \Gamma_c) dV \quad (25)$$

Conservation of Liquid Mass

$$\int_V [\alpha_f \frac{\partial \rho_f}{\partial t} + \rho_f \frac{\partial \alpha_f}{\partial t}] dV = -\int_S \alpha_f \rho_f \bar{v}_f \cdot d\bar{S} - \int_V (\Gamma_{ig} + \Gamma_w + \Gamma_c) dV \quad (26)$$

Balance of Vapor Internal Energy

$$\int_V [\alpha_g \rho_g \frac{\partial u_g}{\partial t} + \alpha_g u_g \frac{\partial \rho_g}{\partial t} + \rho_g u_g \frac{\partial \alpha_g}{\partial t}] dV = -\int_S \alpha_g \rho_g u_g \bar{v}_g \cdot d\bar{S} - \int_V P \frac{\partial \alpha_g}{\partial t} dV -$$

$$\int_S P \alpha_g \bar{v}_g \cdot d\bar{S} + \int_V (\Gamma_{ig} h_g^{\circ} + \Gamma_w h_{wg}^{`} + \Gamma_c h_{cg}^{`} + Q_{wg} + Q_{ig} - Q_{gf} + \alpha_g \rho_g FWG v_g^2) dV \quad (27)$$

Balance of Liquid Internal Energy

$$\int_V [\alpha_f \rho_f \frac{\partial u_f}{\partial t} + \alpha_f u_f \frac{\partial \rho_f}{\partial t} + \rho_f u_f \frac{\partial \alpha_f}{\partial t}] dV = -\int_S \alpha_f \rho_f u_f \bar{v}_f \cdot d\bar{S} - \int_V P \frac{\partial \alpha_f}{\partial t} dV - \int_S P \alpha_f \bar{v}_f \cdot d\bar{S} - \int_V (\Gamma_{ig} h_f^{\circ} + \Gamma_w h_{wf}^{`} + \Gamma_c h_{cf}^{`} - Q_{wf} - Q_{if} - Q_{gf} - \alpha_f \rho_f FWF v_f^2) dV \quad (28)$$

The integral parts in Equations 24 through 28 are approximated by a difference approximation for the time derivatives and using old information for the factors of the time derivatives. Therefore, applying the differentiation of product rules is not done in the conservative method and this is the first difference between the non-conservative and conservative methods. Several general guidelines were followed in developing numerical approximations Equations 29-33 from Equations 24 through 28 (NSAD, 2001). They are:

- Mass and energy are kept consistent and conservative by the numerical scheme, which means both mass and energy are convected from the same cell, and each is evaluated at the old time level (m)
- Implicit evaluation (m+1) is used for the velocity in order to achieve fast execution speed.

Conservation of Mass of Non-condensable Gases in Non-conservative Numerical Approximation Form

$$\frac{V}{\Delta t}\left[(\alpha_g \rho_g)^m \Delta X_n + (\alpha_g X_n)^m \Delta(\rho_g) + (\rho_g X_n)^m \Delta(\alpha_g)\right] = \sum_{j=T_i} (\alpha_g \rho_g X_n)_j^m \bar{v}_{gj}^{m+1} S_j - \sum_{j=F_i} (\alpha_g \rho_g X_n)_j^m \bar{v}_{gj}^{m+1} S_j \quad (29)$$

Conservation of Vapor Mass in Non-conservative Numerical Approximation Form

$$\frac{V}{\Delta t}\left[\left(\alpha_g\right)^m\Delta\left(\rho_g\right)+\left(\rho_g\right)^m\Delta\left(\alpha_g\right)\right]=\left[\sum_{j=T_i}\left(\alpha_g\rho_g\right)_j^m\bar{v}_{gj}^{m+1}S_j-\sum_{j=F_i}\left(\alpha_g\rho_g\right)_j^m\bar{v}_{gj}^{m+1}S_j\right]+$$

$$V(\Gamma_{ig}^{m+1}+\Gamma_w^{m+1}+\Gamma_c^{m+1}) \quad (30)$$

Conservation of Liquid Mass in Non-conservative Numerical Approximation Form

$$\frac{V}{\Delta t}\left[\left(\alpha_f\right)^m\Delta\left(\rho_f\right)+\left(\rho_f\right)^m\Delta\left(\alpha_f\right)\right]=\left[\sum_{j=T_i}\left(\alpha_f\rho_f\right)_j^m\bar{v}_{fj}^{m+1}S_j-\sum_{j=F_i}\left(\alpha_f\rho_f\right)_j^m\bar{v}_{fj}^{m+1}S_j\right]-$$

$$V(\Gamma_{ig}^{m+1}+\Gamma_w^{m+1}+\Gamma_c^{m+1}) \quad (31)$$

Balance of Vapor Internal Energy in Non-conservative Numerical Approximation Form

$$\frac{V}{\Delta t}\{\left(\alpha_g\rho_g\right)^m\Delta u_g+\left(\alpha_g u_g\right)^m\Delta\left(\rho_g\right)+[\left(\rho_g u_g\right)^m+P^m]\Delta\left(\alpha_g\right)\}=$$

$$[\sum_{j=T_i}\left(\alpha_g\rho_g u_g\right)_j^m\bar{v}_{gj}^{m+1}S_j-\sum_{j=F_i}\left(\alpha_g\rho_g u_g\right)_j^m\bar{v}_{gj}^{m+1}S_j]-P^m[\sum_{j=T_i}{\alpha_{gj}}^m\bar{v}_{gj}^{m+1}S_j-$$

$$\sum_{j=F_i}{\alpha_{gj}}^m\bar{v}_{gj}^{m+1}S_j]+V[\Gamma_{ig}^{m+1}h_g^{\circ}+\Gamma_w^{m+1}h_{wg}^{`}+\Gamma_c^{m+1}h_{cg}^{`}+Q_{wg}^{m+1}+Q_{ig}^{m+1}-Q_{gf}^{m+1}+$$

$$(\alpha_g\rho_g FWGv_g^2)^m] \quad (32)$$

Balance of Liquid Internal Energy in Non-conservative Numerical Approximation Form

$$\frac{V}{\Delta t}\{\left(\alpha_f\rho_f\right)^m\Delta u_f+\left(\alpha_f u_f\right)^m\Delta\left(\rho_f\right)+[\left(\rho_f u_f\right)^m+P^m]\Delta\left(\alpha_f\right)\}=$$

$$[\sum_{j=T_i}\left(\alpha_f\rho_f u_f\right)_j^m\bar{v}_{fj}^{m+1}S_j-\sum_{j=F_i}\left(\alpha_f\rho_f u_f\right)_j^m\bar{v}_{fj}^{m+1}S_j]-P^m[\sum_{j=T_i}{\alpha_{fj}}^m\bar{v}_{fj}^{m+1}S_j-$$

$$\sum_{j=F_i}{\alpha_{fj}}^m\bar{v}_{fj}^{m+1}S_j]-V[\Gamma_{ig}^{m+1}h_f^{\circ}+\Gamma_w^{m+1}h_{wf}^{`}+\Gamma_c^{m+1}h_{cf}^{`}-Q_{wf}^{m+1}-Q_{if}^{m+1}-Q_{gf}^{m+1}-$$

$$(\alpha_f\rho_f FWFv_f^2)^m] \quad (33)$$

The forward Euler approximation to the time derivative of the quantities is the simple difference between the new and old time values of the quantity divided by the time difference. The subscribe j stands for junction index. Subscribes T and F stand for ‘to’ and ‘from’ junction index separately. Symbol S represents junction flow area. In the RELAP5 equations, the time derivative of the convected quantities is the sum of the time derivative approximation for each factor times the product of the old values of other factors. In the conservative method, time derivative approximation is applied to the convected quantity as a unit and they are called macroscopic quantities (USNRC, TRACE V5.0).

Chapter 4: Conservation Equations in Conservative Forms

Numerical approaches are different for conservative and non-conservative methods when applying derivatives in conservative equations (Equations 6-10). In non-conservative approximation used in current version of RELAP5 (NSAD, 2001), the derivative of $(\alpha_g, \alpha_f, \rho_g, \rho_f, u_g, u_f, X_n)$ involves the multiplication of each term's derivative. However, in the conservative approximation, the approximation to differentiation is applied to the convective quantities (macroscopic quantities), that is, the product terms $\left(\widehat{\alpha_g \rho_g X_n}\right)$, $\left(\widehat{\alpha_g \rho_g u_g}\right)$, $\left(\widehat{\alpha_f \rho_f u_f}\right)$, $\left(\widehat{\alpha_g \rho_g}\right)$, and $\left(\widehat{\alpha_f \rho_f}\right)$. These convective quantities now become unknowns in the resultant set of simultaneous equations. To clearly indicate the convective terms as opposed to the factors in the convective terms, the factors with a curved mark placed above the factors are used as a symbol for the convective quantities.

Equations 34-38 demonstrate mass, momentum and energy conservation equations in conservative numerical approximation forms.

Conservation of Mass of Non-condensable Gases in Conservative Numerical Approximation Form

$$\frac{V}{\Delta t}\left[\Delta\left(\widehat{\alpha_g \rho_g X_n}\right)\right] = \sum_{j=T_i}\left(\alpha_g \rho_g X_n\right)_j^m \bar{v}_{gj}^{m+1} S_j - \sum_{j=F_i}\left(\alpha_g \rho_g X_n\right)_j^m \bar{v}_{gj}^{m+1} S_j \qquad (34)$$

Conservation of Vapor Mass in Conservative Numerical Approximation Form

$$\frac{V}{\Delta t}\left[\Delta\left(\widehat{\alpha_g \rho_g}\right)\right] - V(\Delta\Gamma_{ig} + \Delta\Gamma_w + \Delta\Gamma_c) +$$

$$\left[\sum_{j=T_i}\left(\alpha_g \rho_g\right)_j^m \bar{v}_{gj}^{m+1} S_j - \sum_{j=F_i}\left(\alpha_g \rho_g\right)_j^m \bar{v}_{gj}^{m+1} S_j\right] = V(\Gamma_{ig}^m + \Gamma_w^m + \Gamma_c^m) \qquad (35)$$

Conservation of Liquid Mass in Conservative Numerical Approximation Form

$$\frac{V}{\Delta t}\left[\Delta\left(\widehat{\alpha_f \rho_f}\right)\right] + V\left(\Delta\Gamma_{ig} + \Delta\Gamma_w + \Delta\Gamma_c\right) +$$

$$\left[\sum_{j=T_i}\left(\alpha_f \rho_f\right)_j^m \bar{v}_{fj}^{m+1} S_j - \sum_{j=F_i}\left(\alpha_f \rho_f\right)_j^m \bar{v}_{fj}^{m+1} S_j\right] = -V(\Gamma_{ig}^m + \Gamma_w^m + \Gamma_c^m) \quad (36)$$

Balance of Vapor Internal Energy in Conservative Numerical Approximation Form

$$\frac{V}{\Delta t}\left[\Delta\left(\widehat{\alpha_g \rho_g u_g}\right)\right] - V\Delta\Gamma_{ig} h_g^{\circ} - V\Delta\Gamma_w h_{wg}^{`} - V\Delta\Gamma_c h_{cg}^{`} - V\Delta Q_{wg} - V\Delta Q_{ig} + V\Delta Q_{gf} +$$

$$\left[\sum_{j=T_i}\left(\alpha_g \rho_g u_g\right)_j^m \bar{v}_{gj}^{m+1} S_j - \sum_{j=F_i}\left(\alpha_g \rho_g u_g\right)_j^m \bar{v}_{gj}^{m+1} S_j\right] - P^m\left[\sum_{j=T_i} {\alpha_{gj}}^m \bar{v}_{gj}^{m+1} S_j - \right.$$

$$\left.\sum_{j=F_i} {\alpha_{gj}}^m \bar{v}_{gj}^{m+1} S_j\right] =$$

$$V[\Gamma_{ig}^m h_g^{\circ} + \Gamma_w^m h_{wg}^{`} + \Gamma_c^m h_{cg}^{`} + Q_{wg}^m + Q_{ig}^m - Q_{gf}^m + (\alpha_g \rho_g FWG v_g^2)^m] \quad (37)$$

Balance of Liquid Internal Energy in Conservative Numerical Approximation Form

$$\frac{V}{\Delta t}\left[\Delta\left(\widehat{\alpha_f \rho_f u_f}\right)\right] + V\Delta\Gamma_{ig} h_f^{\circ} + V\Delta\Gamma_w h_{wf}^{`} + V\Delta\Gamma_c h_{cf}^{`} - V\Delta Q_{wf} - V\Delta Q_{if} - V\Delta Q_{gf} +$$

$$\left[\sum_{j=T_i}\left(\alpha_f \rho_f u_f\right)_j^m \bar{v}_{fj}^{m+1} S_j - \sum_{j=F_i}\left(\alpha_f \rho_f u_f\right)_j^m \bar{v}_{fj}^{m+1} S_j\right] - P^m\left[\sum_{j=T_i} {\alpha_{fj}}^m \bar{v}_{fj}^{m+1} S_j - \right.$$

$$\left.\sum_{j=F_i} {\alpha_{fj}}^m \bar{v}_{fj}^{m+1} S_j\right] =$$

$$-V[\Gamma_{ig}^m h_f^{\circ} + \Gamma_w^m h_{wf}^{`} + \Gamma_c^m h_{cf}^{`} - Q_{wf}^m - Q_{if}^m - Q_{gf}^m - (\alpha_f \rho_f FWF v_f^2)^m] \quad (38)$$

The five product quantities are essentially additional unknowns, and five additional algebraic relationships are required to solve balance equations. The additional relationships are the algebraic expressions defining the product quantities. When the liquid or vapor phase is not present in a volume, indefinite results can arise, and provisions must be provided for those situations. The algebraic expressions are presented here and they include the linearized

approximations to the expressions, which are the expressions for the indefinite processing. For example, the definition of non-condensable mass fraction is given by Equations 39 and 40.

Non-condensable Mass Fraction Definition

$$X_n = \frac{(\widehat{\alpha_g \rho_g X_n})}{(\widehat{\alpha_g \rho_g})}, \text{ if } (\widehat{\alpha_g \rho_g})^{m+1} > 0 \tag{39}$$

$$X_n = 0, \qquad \text{if } (\widehat{\alpha_g \rho_g})^{m+1} = 0 \tag{40}$$

Newton-Raphson method is used to obtain the linearized approximation for algebraic equations. Equations 43 and 44 are plugged into Newton-Raphson Equation 41 to result the approximation equations 45-46 for the non-condensable mass fraction definition.

$$-\frac{\partial}{\partial \bar{y}} F(\bar{y}^m) \cdot \Delta \bar{y} = F(\bar{y}^m) \tag{41}$$

, where $\Delta \bar{y} = \bar{y}^{m+1} - \bar{y}^m$ and

$$F(\bar{y}^m) = F\left(X_n^m, \left(\widehat{\alpha_g \rho_g X_n}\right)^m, \left(\widehat{\alpha_g \rho_g}\right)^m\right) = X_n^m - \frac{(\widehat{\alpha_g \rho_g X_n})^m}{(\widehat{\alpha_g \rho_g})^m} \tag{42}$$

, so its derivative becomes

$$-\frac{\partial}{\partial \bar{y}} F(\bar{y}^m) = -[1, -\frac{1}{(\widehat{\alpha_g \rho_g})^m}, \frac{(\widehat{\alpha_g \rho_g X_n})^m}{[(\widehat{\alpha_g \rho_g})^m]^2}] \tag{43}$$

$$\Delta \bar{y} = [\Delta X_n^m, \Delta\left(\widehat{\alpha_g \rho_g X_n}\right)^m, \Delta\left(\widehat{\alpha_g \rho_g}\right)^m] \tag{44}$$

Then, the approximation Equation 41 becomes

$$\Delta X_n - \frac{\Delta(\widehat{\alpha_g\rho_g}X_n)}{(\widehat{\alpha_g\rho_g})^m} + \frac{(\widehat{\alpha_g\rho_g}X_n)^m\Delta(\widehat{\alpha_g\rho_g})}{\left[(\widehat{\alpha_g\rho_g})^m\right]^2} = \frac{(\widehat{\alpha_g\rho_g}X_n)^m}{(\widehat{\alpha_g\rho_g})^m} - X_n^m$$

, if $(\widehat{\alpha_g\rho_g})^{m+1} > 0$ (45)

$$\Delta X_n = 0$$

, if $(\widehat{\alpha_g\rho_g})^{m+1} = 0$ (46)

Vapor internal energy definition is given by Equations 47 and 48. Equations 49 and 50 are derived with Newton-Raphson method [Equation 41] from Equations 47 and 48 in the same manner of non-condensable mass fraction.

Vapor Internal Energy Definition

$$u_g = \frac{(\widehat{\alpha_g\rho_g u_g})}{(\widehat{\alpha_g\rho_g})}, \qquad \text{if } (\widehat{\alpha_g\rho_g})^{m+1} > 0 \tag{47}$$

$$u_g = F_{sgu}(T_s), \qquad \text{if } (\widehat{\alpha_g\rho_g})^{m+1} = 0 \tag{48}$$

Vapor Internal Energy Approximations

$$\Delta u_g - \frac{\Delta\left(\widehat{\alpha_g\rho_g u_g}\right)}{\left(\widehat{\alpha_g\rho_g}\right)^m} + \frac{\left(\widehat{\alpha_g\rho_g u_g}\right)^m \Delta\left(\widehat{\alpha_g\rho_g u_g}\right)}{\left[\left(\widehat{\alpha_g\rho_g}\right)^m\right]^2} = \frac{\left(\widehat{\alpha_g\rho_g u_g}\right)^m}{\left(\widehat{\alpha_g\rho_g}\right)^m} - u_g^m$$

, if $(\widehat{\alpha_g\rho_g})^{m+1} > 0$ (49)

$$\Delta u_g - \left.\frac{dF_{sgu}}{dT_s}\right|_m \Delta T_s = F_{sgu}(T_s^m) - u_g^m$$

, if $(\widehat{\alpha_g\rho_g})^{m+1} = 0$ (50)

Equations 51 and 52 give the definition of liquid internal energy. Equations 53 and 54 give the numerical approximation forms of liquid internal energy.

Liquid Internal Energy Definition

$$u_f = \frac{(\widehat{\alpha_f\rho_f u_f})}{(\widehat{\alpha_f\rho_f})}, \qquad \text{if } (\widehat{\alpha_f\rho_f})^{m+1} > 0 \tag{51}$$

$$u_f = F_{sfu}(T_s), \qquad \text{if } (\widehat{\alpha_f\rho_f})^{m+1} = 0 \tag{52}$$

Liquid Internal Energy Approximations

$$\Delta u_f - \frac{\Delta(\widehat{\alpha_f\rho_f u_f})}{(\widehat{\alpha_f\rho_f})^m} + \frac{(\widehat{\alpha_f\rho_f u_f})^m \Delta(\widehat{\alpha_f\rho_f u_f})}{\left[(\widehat{\alpha_f\rho_f})^m\right]^2} = \frac{(\widehat{\alpha_f\rho_f u_f})^m}{(\widehat{\alpha_f\rho_f})^m} - u_f^m$$

, if $(\widehat{\alpha_f\rho_f})^{m+1} > 0$ (53)

$$\Delta u_f - \left.\frac{dF_{sfu}}{dT_s}\right|_{mi} \Delta T_s = F_{sfu}(T_s^m) - u_f^m$$

, if $(\widehat{\alpha_f\rho_f})^{m+1} = 0$ (54)

Equations 45-46, 49-50, and 53-54 are not needed for the non-conservative form of differential, but they are necessary for the proposed conservative equations due to the extra unknowns introduced in conservative form. Since we introduce five new unknowns, we need two more relationships in order to close the system of the equations. These two relationships are embedded in liquid/vapor void fraction [Equation 55]. Following twelve thermodynamic relations are the rest of constitutive equations for conservative numerical approximation.

Liquid and vapor void fraction relationship used for conservative form is presented in Equation 55 and its approximation [Equation 56] is derived by applying Newton-Raphson method [Equation 41].

Liquid and Vapor Void Fractions Relationship

$$\alpha_g + \alpha_f = \frac{\widehat{(\alpha\rho)_g}}{\rho_g} + \frac{\widehat{(\alpha\rho)_f}}{\rho_f} = 1 \quad (55)$$

Liquid and Vapor Void Fractions Approximation

$$\frac{\Delta\widehat{(\alpha\rho)}_g}{\rho_g^m} - \frac{\widehat{(\alpha\rho)}_g^m \Delta\rho_g}{\left(\rho_g^m\right)^2} + \frac{\Delta\widehat{(\alpha\rho)}_f}{\rho_f^m} - \frac{\widehat{(\alpha\rho)}_f^m \Delta\rho_f}{\left(\rho_f^m\right)^2} = 0 \tag{56}$$

The seventh and eighth constitutive equations are state equation for vapor density [Equation 57-58] and state equation for vapor temperature [Equation 61-62]. Their approximation equations are Equations 59-60 and 63-64 separately.

Equations of State for Vapor Density

$$\rho_g = F_{\rho g}(P, u_g, X_n), \qquad \text{if } (\widehat{\alpha_g \rho_g})^{m+1} > 0 \tag{57}$$

$$\rho_g = F_{s\rho g}(P), \qquad \text{if } (\widehat{\alpha_g \rho_g})^{m+1} = 0 \tag{58}$$

Equations of State for Vapor Density Approximations

$$-\left.\frac{\partial F_{\rho g}}{\partial X_n}\right|_m \Delta X_n - \left.\frac{\partial F_{\rho g}}{\partial u}\right|_m \Delta u_g + \Delta\rho_g - \left.\frac{\partial F_{\rho g}}{\partial P}\right|_m \Delta P = 0$$

, if $(\widehat{\alpha_g \rho_g})^{m+1} > 0$ (59)

$$\Delta\rho_g - \left.\frac{dF_{s\rho g}}{dP}\right|_m \Delta P = F_{s\rho g}(P^m) - \rho_g^m$$

, if $(\widehat{\alpha_g \rho_g})^{m+1} = 0$ (60)

Equations of State for Vapor Temperature

$$T_g = F_{Tg}(P, u_g, X_n), \qquad \text{if } (\widehat{\alpha_g \rho_g})^{m+1} > 0 \tag{61}$$

$$T_g = F_{sT}(P), \qquad \text{if } (\widehat{\alpha_g \rho_g})^{m+1} = 0 \tag{62}$$

Equations of State for Vapor Temperature Approximations

$$-\frac{\partial F_{Tg}}{\partial X_n}\Big|_m \Delta X_{ni} - \frac{\partial F_{Tg}}{\partial u}\Big|_m \Delta u_g + \Delta T_g - \frac{\partial F_{Tg}}{\partial P}\Big|_m \Delta P = 0$$

$$\text{, if } (\widehat{\alpha_g \rho_g})^{m+1} > 0 \tag{63}$$

$$\Delta T_g - \frac{dF_{sTg}}{dP}\Big|_m \Delta P = F_{sTg}(P^m) - T_g^m$$

$$\text{, if } (\widehat{\alpha_g \rho_g})^{m+1} = 0 \tag{64}$$

Equations 65 and 66 are the state equations of liquid density. Equations 67 and 68 are their approximation forms derived from Equations 41.

Equations of State for Liquid Density

$$\rho_f = F_{\rho f}(P,\ u_f), \qquad \text{if } (\widehat{\alpha_f \rho_f})^{m+1} > 0 \tag{65}$$

$$\rho_f = F_{s\rho f}(P), \qquad \text{if } (\widehat{\alpha_f \rho_f})^{m+1} = 0 \tag{66}$$

Equations of State for Liquid Density Approximations

$$-\frac{\partial F_{\rho f}}{\partial u}\Big|_m \Delta u_f + \Delta\rho_f - \frac{\partial F_{\rho f}}{\partial P}\Big|_m \Delta P = 0$$

, if $(\widehat{\alpha_f\rho_f})^{m+1} > 0$ (67)

$$\Delta\rho_f - \frac{dF_{s\rho f}}{dP}\Big|_m \Delta P = F_{s\rho f}(P^m) - \rho_f^m$$

, if $(\widehat{\alpha_f\rho_f})^{m+1} = 0$ (68)

Equations 69 and 70 are the state equations of liquid density. Equations 71 and 72 are approximation forms of equations of state for liquid temperature.

Equations of State for Liquid Temperature

$$T_f = F_{Tf}(P, u_f), \qquad \text{if } (\widehat{\alpha_f\rho_f})^{m+1} > 0 \tag{69}$$

$$T_f = F_{sT}(P), \qquad \text{if } (\widehat{\alpha_f\rho_f})^{m+1} = 0 \tag{70}$$

Equations of State for Liquid Temperature Approximations

$$-\frac{\partial F_{Tf}}{\partial u}\Big|_m \Delta u_f + \Delta T_f - \frac{\partial F_{Tf}}{\partial P}\Big|_m \Delta P = 0$$

, if $(\widehat{\alpha_f\rho_f})^{m+1} > 0$ (71)

$$\Delta T_f - \frac{dF_{sTf}}{dP}\Big|_m \Delta P = F_{sTf}(P^m) - T_f^m$$

, if $(\widehat{\alpha_f\rho_f})^{m+1} = 0$ (72)

Equations of saturation temperature corresponding to partial pressure of water vapor are shown from Equations 73 through 74. Their numerical approximation forms are Equations 75 and 76.

Equations of State for Saturation Temperature Corresponding to Partial Pressure of Water Vapor

$$T_s = F_{sT}(P_s), \quad \text{if } X_n > 0 \tag{73}$$

$$T_s = T_T, \quad \text{if } X_n = 0 \tag{74}$$

Equations of State for Saturation Temperature Corresponding to Partial Pressure of Water Vapor Approximations

$$-\frac{dF_{sT}}{dP_s}\Big|_m \Delta P_s + \Delta T_s = F_{sT}(P_s^m) - T_s, \text{ if } X_n > 0 \tag{75}$$

$$\Delta T_s = \Delta T_T, \quad \text{if } X_n = 0 \tag{76}$$

Equations of saturation temperature corresponding to total pressure of water vapor are shown from Equations 77 through 78. Their numerical approximation forms are shown in Equations 79 and 80.

Equation of State for Saturation Temperature Corresponding to Total Pressure

$$T_T = F_{sT}(P) \tag{77}$$

Equation of State for Saturation Temperature Corresponding to Total Pressure Approximation

$$-\frac{\partial F_{sT}}{\partial P}\Big|_m \Delta P + \Delta T_f = F_{sT}(P^m) - T_T^m \quad (78)$$

The interface transfer quantities including both mass and energy transfers are presented below. The definition of interface mass transfer is shown in Equation 79 and Equation 80 gives its numerical approximation form.

Interface Mass Transfer

$$\Gamma_{ig} = -\frac{H_{ig}[T_s - T_g] + H_{if}[T_s - T_f]}{h_g^\circ - h_f^\circ} = F_{ig}(T_s,\ T_g,\ T_f) \quad (79)$$

Interface Mass Transfer Approximation

$$-\frac{H_{ig}\Delta T_g + H_{if}\Delta T_f - [H_{ig} + H_{if}]\Delta T_s}{h_g^\circ - h_f^\circ} + \Delta\Gamma_{ig} = F_{ig}\left({T_s}^m,\ T_g^m,\ T_f^m\right) - \Gamma_{ig}^m \quad (80)$$

The definition of interface energy transfer is shown in Equation 81 and Equation 82 gives its numerical approximation form.

Interface Energy Transfer

$$\Gamma_e = -\frac{h_f^\circ H_{ig}[T_s - T_g] + h_g^\circ H_{if}[T_s - T_f]}{h_g^\circ - h_f^\circ} = F_e(T_s,\ T_g,\ T_f) \quad (81)$$

Interface Energy Transfer Approximation

$$-\frac{\overset{\circ}{h_f}H_{ig}\Delta T_g+\overset{\circ}{h_g}H_{if}\Delta T_f-\left[\overset{\circ}{h_f}H_{ig}+\overset{\circ}{h_g}H_{if}\right]\Delta T_s}{\overset{\circ}{h_g}-\overset{\circ}{h_f}}+\Delta\Gamma_e=F_e\left({T_s}^m,\ T_g^m,\ T_f^m\right)-\Gamma_e^m \tag{82}$$

Definitions and their approximations of mass transfers due to wall are presented in Equation 83 through Equation 86. Flashing is mass transfer from liquid to vapor; condensations transfers mass from vapor to liquid phase.

Mass Transfer at Wall Due to Flashing

$$\Gamma_w=\Gamma_{wfo}+\Gamma_{wff}\Delta T_f+\Gamma_{wfg}\Delta T_g+\Gamma_{wfspt}\Delta T_T+\Gamma_{wfspp}\Delta T_s \tag{83}$$

Mass Transfer at Wall Due to Flashing Approximation

$$\Delta\Gamma_w-\Gamma_{wg}\Delta T_g-\Gamma_{wf}\Delta T_f-\Gamma_{ws}\Delta T_s-\Gamma_{wT}\Delta T_T=T_w^0-T_w^m \tag{84}$$

Mass Transfer at Wall Due to Condensation

$$\Gamma_c=\Gamma_{wgo}+\Gamma_{wgf}\Delta T_f+\Gamma_{wgg}\Delta T_g+\Gamma_{wgspt}\Delta T_T+\Gamma_{wgspp}\Delta T_s \tag{85}$$

Mass Transfer at Wall Due to Condensation Approximation

$$\Delta\Gamma_c-\Gamma_{cg}\Delta T_g-\Gamma_{cf}\Delta T_f-\Gamma_{cs}\Delta T_s-\Gamma_{cT}\Delta T_T=T_c^0-T_c^m \tag{86}$$

Finally, definitions of heat transfers due to wall are presented. The definition of wall heat transfer to vapor is shown in Equation 87 and Equation 88 gives its numerical approximation form.

Wall Heat Transfer to Vapor

$$Q_{wg} = Q_{wgo} + Q_{wgf}\Delta T_f + Q_{wgg}\Delta T_g + Q_{wgspt}\Delta T_T + Q_{wgspp}\Delta T_s \quad (87)$$

Wall Heat Transfer to Vapor Approximation

$$\Delta q_g - q_{gg}\Delta T_g - q_{gf}\Delta T_f - q_{gs}\Delta T_s - q_{gT}\Delta T_T = q_g^0 - q_g^m \quad (88)$$

The definition of wall heat transfer to liquid is shown in Equation 89 and Equation 90 gives numerical approximation form of wall heat transfer to liquid.

Wall Heat Transfer to Liquid

$$Q_{wf} = Q_{wfo} + Q_{wff}\Delta T_f + Q\Gamma_{wfg}\Delta T_g + Q_{wfspt}\Delta T_T + Q_{wfspp}\Delta T_s \quad (89)$$

Wall Heat Transfer to Liquid Approximation

$$\Delta q_f - q_{fg}\Delta T_g - q_{ff}\Delta T_f - q_{fs}\Delta T_s - q_{fT}\Delta T_T = q_f^0 - q_f^m \quad (90)$$

Chapter 5: Solution Strategies of the Non-conservative and Conservative Method

Before introducing the solution strategy for the new conservative method, the semi-implicit advancement solution strategy of the non-conservative method in current RELAP5 is briefly described first.

The numerical approximation to the momentum equations results in two equations per junction, involving only the liquid and vapor velocities for the junction and the pressures for the two volumes connected by each junction. Using the 2 by 2 matrices from the two equations per junction, expressions for the liquid and vapor velocities in terms of the pressures from the connected volumes can be obtained. The numerical approximations for the other conservations equations result in five equations per volume derived from the partial differential equations plus thirteen equations from the algebraic relationships. Using algebraic substitutions, variables can be eliminated until only five equations per volume remain, involving volume pressure, vapor void fraction, liquid and vapor internal energies, and non-condensable mass fraction. The submitters involving the remaining five equations per volume is factored into lower and upper submitters, the submitters manipulated to obtain the inverse elements for the row of the matrix defining the pressure. Using the inverse elements, an expression can be obtained for one equation for each volume involving the pressure and the velocities from the attached junctions. The velocity expressions obtained from the momentum equations are used to eliminate the velocities in the pressure equation obtained from the inverse elements. This results in a system of equations, one per volume, involving only volume pressures. The resulting matrix is solved for pressures using a sparse matrix routine. The number of equations in the sparse matrix is one equation for each volume and the nonusers in the sparse matrix are the diagonal element plus an off-diagonal element

for each volume. The pressures are back substituted into the expressions from the momentum equations to obtain velocities, and pressures and velocities are back substituted into the other four volume elations to obtain the remaining volume quantities (NSAD, 2001).

The conservative form of the conservation equations should be able to be solved in a similar manner to that for the non-conservative form. However, comparing the non-conservative form, the conservative form of the differential equations introduces five new unknowns, which requires five extra algebraic equations to solve the simultaneous equations. Therefore, there are twenty-one unknowns in total for conservative volume mass and energy sub-matrices. Those unknowns are the convective quantity for non-condensable mass fraction (kg/m^3), the convective quantity for vapor density (kg/m^3), the convective quantity for liquid density (kg/m^3), the convective quantity for vapor internal energy (J/m^3), the convective quantity for liquid internal energy (J/m^3), non-condensable mass fraction , vapor internal energy (J/m^3), liquid internal energy (J/m^3), liquid density (kg/m^3), vapor density (kg/m^3), total pressure (Pa), vapor temperature (K), liquid temperature (K), the saturation temperature corresponding to partial pressure of water vapor (K), the saturation temperature corresponding to total pressure (K), the interface mass transfer (kg/m^3s), the interface energy transfer associated with interface mass transfer (W/m^3), the flashing rate at wall (kg/m^3s), the condensing rate at wall (kg/m^3s), the wall heat transfer to vapor (W/m^3), the wall heat transfer to liquid (W/m^3) (Fu, Z., Aydogan, F., Wagner, R., 2014).

The corresponding twenty one volume-related equations are sixteen closure equations and five conservation equations. These five conservation equations include the conservation of mass of non-condensable gases, the conservation of vapor mass, the conservation of liquid mass, the conservation of vapor internal energy, and the conservation of liquid internal

energy. Sixteen closure equations include definitions of quality, vapor internal energy, liquid internal energy, vapor density, liquid density, void fraction, vapor temperature, liquid temperature, the saturation temperature corresponding to partial pressure, the saturation temperature corresponding to total pressure, interface mas transfer, interface energy exchange, the wall mass transfer to vapor, the wall mass transfer to liquid, the wall heat transfer to vapor, and the wall heat transfer to liquid (Fu, Z., Aydogan, F., Wagner, R., 2014).

Unlike non-conservative solution strategy, which solves a 5 by 5 matrix and closure equations separately, the conservative approach simply places all twenty one equations for each volume and two monument equations per junction into a single sparse matrix and it uses the sparse matrix routines to obtain the solutions.

Chapter 6: Matrix Structure of the System of Equations

The hydrodynamic volumes and junctions used in a RELAP5 simulation are divided into hydrodynamic systems. Fluid in a system can only move within that system. The primary and secondary systems in a reactor power would be separate systems in a RELAP5 simulation. If a steam generator tube is modeled to allow a tube rupture by inserting a valve between the inside and outside of the generator tube, the primary and secondary systems now become one system whether the valve is opened or closed. Each hydrodynamic system is advanced separately. This is, the simultaneous equations and their systems are built and solved separately. The hydrodynamic systems can be linked thermally, and the hydrodynamic and heat conduction simultaneous equations are linked. But this linkage is done with a quite small impact on the either the hydrodynamic or heat conduction solution procedures.

For the non-conservative form of the conservation equations, the number of simultaneous equations in a hydrodynamic system is 19 * number of volumes + 2 * the number of junctions. For moderately sized system with 100 volumes and 100 junctions, the number of simultaneous equation would be 2100. The previous section shows that, for the conservative form of the conservation equations, the number of simultaneous equations is 21 * number of volumes + 2 * number of junction. The number of simultaneous equations for the conservative form of the moderately sized problem is 2300, about a 10 percent increase.

This section presents the structure of matrix in conservative form and lists all the coefficients in five conservation equations and sixteen constitutive equations. Mass and energy conservation equations and closure equations form a 21 by 21 nonzero pattern for mass-energy sub-matrix for each volume in order to solve twenty one unknowns associated volume quantities. The diagonal sub-matrix for conservation of mass and energy equations is

called matrix A_{vv} (Figure 2). The equation names are presented in the rows and the unknowns are in columns.

		(αρX)g	(αρ)g	(αρ)f	(αρμ)g	(αρμ)f	Xn	ug	uf	ρg	ρf	P	Tg	Tf	Tsp	Tst	Γig	Γe	Γw	Γc	Qwg	Qwf
		1	2	3	4	5	6	7	8	9	10	11	12	13	14	15	16	17	18	19	20	21
1	Conservation of noncondensable gases	1,1																				
2	Conservation of vapor mass		2,2														2,16		2,18	2,19		
3	Conservation of liquid Mass			3,3													3,16		3,18	3,19		
4	Conservation of vapor internal energy				4,4													4,17	4,18	4,19	4,20	
5	Conservation of liquid internal energy					5,5												5,17	5,18	5,19		5,21
6	Mass fraction of noncondensable gases	6,1	6,2				6,6															
7	Vapor internal energy		7,2		7,4			7,7														
8	Liquid internal energy			8,3		8,5			8,8													
9	vapor density						9,6	9,7		9,9		9,11										
10	liquid density								10,8		10,10	10,11										
11	void fraction		11,2	11,3						11,9	11,10	11,11										
12	vapor temperature						12,6	12,7				12,11	12,12									
13	liquid temperature								13,8			13,11		13,13								
14	saturation temperature corresponding to paitial pressure						14,6	14,7				14,11			14,14							
15	saturation temperature corresponding to total pressure											15,11				15,15						
16	interface mass transfer												16,12	16,13	16,14		16,16					
17	interface energy exchange												17,12	17,13	17,14			17,17				
18	wall mass transfer to vapor												18,12	18,13	18,14	18,15			18,18			
19	wall mass transfer to liquid												19,12	19,13	19,14	19,15				19,19		
20	wall heat transfer to vapor												20,12	20,13	20,14	20,15					20,20	
21	wall heat transfer to liquid												21,12	21,13	21,14	21,15						21,21

Figure 2: Structure of Volume Matrix A_{vv}

The matrix above is a sparse matrix, which means most of elements in matrix are zeroes. However, the element filled with numbers above have non-zero coefficients. Each pair of numbers represents row and column indexes. A matrix solver is used to solve vector x in operation $A_{vv}x=b$ and x contains the increments of twenty-one volume quantities (Figure 3). Moreover, A_{vv} is a sub-matrix of A and its coefficients are listed in Equations 91 to 150 and vector b equals to zero.

$$x = \begin{bmatrix} \Delta(\alpha_g \widehat{\rho}_g X) \\ \Delta(\alpha_g \widehat{\rho}_g) \\ \Delta(\alpha_f \widehat{\rho}_f) \\ \Delta(\alpha_g \widehat{\rho}_g u_g) \\ \Delta(\alpha_f \widehat{\rho}_f u_f) \\ \Delta X_n \\ \Delta u_g \\ \Delta u_f \\ \Delta \rho_g \\ \Delta \rho_f \\ \Delta P \\ \Delta T_g \\ \Delta T_f \\ \Delta T_{sp} \\ \Delta T_{sT} \\ \Delta \Gamma_{ig} \\ \Delta \Gamma_e \\ \Delta \Gamma_w \\ \Delta \Gamma_c \\ \Delta Q_{wg} \\ \Delta Q_{wf} \end{bmatrix} = \begin{bmatrix} (\alpha_g \widehat{\rho}_g X_n)^{m+1} - (\alpha_g \widehat{\rho}_g X_n)^m \\ (\alpha_g \widehat{\rho}_g)^{m+1} - (\alpha_g \widehat{\rho}_g)^m \\ (\alpha_f \widehat{\rho}_f)^{m+1} - (\alpha_f \widehat{\rho}_f)^m \\ (\alpha_g \widehat{\rho}_g u_g)^{m+1} - (\alpha_g \widehat{\rho}_g u_g)^m \\ (\alpha_f \widehat{\rho}_f u_f)^{m+1} - (\alpha_f \widehat{\rho}_f u_f)^m \\ X_n^{m+1} - X_n^m \\ u_g^{m+1} - u_g^m \\ u_f^{m+1} - u_f^m \\ \rho_g^{m+1} - \rho_g^m \\ \rho_f^{m+1} - \rho_f^m \\ P^{m+1} - P^m \\ T_g^{m+1} - T_g^m \\ T_f^{m+1} - T_f^m \\ T_{sp}^{m+1} - T_{sp}^m \\ T_{sT}^{m+1} - T_{sT}^m \\ \Gamma_{ig}^{m+1} - \Gamma_{ig}^m \\ \Gamma_e^{m+1} - \Gamma_e^m \\ \Gamma_w^{m+1} - \Gamma_w^m \\ \Gamma_c^{m+1} - \Gamma_c^m \\ Q_{wg}^{m+1} - Q_{wg}^m \\ Q_{wf}^{m+1} - Q_{wf}^m \end{bmatrix}$$

Figure 3: Vector x Containing Increments in Volume Quantities

The vector x is solved for the increment of each volume quantity and they are added into previous values in order to get new time values. There are total eighty-one nonzero coefficients. Twenty-one diagonal elements have coefficient one; other nonzero coefficients in matrix A_{vv} are listed below.

The first equation in matrix A_{vv} is the conservation of non-condensable gases, which has only one non-zero element at row one and column one as shown in Figure 2. The second row in matrix A_{vv} represents conservation of vapor mass, which has unknown variables of convective quantity for vapor density (column 2), interface mass transfer (column 16),

flashing rate at wall (column 18), and condensing rate at wall (column 19). Its off-diagonal element coefficients are presented in Equations 91 through 93.

Coefficients in Conservation of Vapor Mass

$$A_{0216} = -\Delta t \quad (91)$$

$$A_{0218} = -\Delta t \quad (92)$$

$$A_{0219} = -\Delta t \quad (93)$$

The third row in A_{vv} is conservation of liquid mass equation. The unknowns in the equation are convective quantity for liquid density (column 3), interface mass transfer (column 16), flashing rate at wall (column 18), and condensing rate at wall (column 19). Their off-diagonal element coefficients are shown in Equations 94 through 96.

Coefficients in Conservation of Liquid Mass

$$A_{0316} = \Delta t \quad (94)$$

$$A_{0318} = \Delta t \quad (95)$$

$$A_{0319} = \Delta t \quad (96)$$

Conservation of vapor internal energy occupies the fourth row of A_{vv}. The unknowns in the equation are convective quantity for vapor internal energy (column 4), interface energy transfer associated with interface mass transfer (column 17), flashing rate at wall (column 18), condensing rate at wall (column 19), and wall heat transfer to vapor (column 20). The off-diagonal coefficients are shown in Equations 97 through 100.

Coefficients in Conservation of Vapor Internal Energy

$$A_{0417} = -\Delta t \quad (97)$$

$$A_{0418} = -h_g \Delta t \quad (98)$$

$$A_{0419} = -h_f \Delta t \quad (99)$$

$$A_{0420} = -\frac{\Delta t}{V} \quad (100)$$

Conservation of liquid internal energy is in fifth row, which includes five unknowns - convective quantity for liquid internal energy (column 5), interface energy transfer associated with interface mass transfer (column 17), flashing rate at wall (column 18), condensing rate at wall (column 19), and wall heat transfer to liquid (column 21). The off-diagonal coefficients are shown in Equations 101 through 104.

Coefficients in Conservation of Liquid Internal Energy

$$A_{0517} = \Delta t \quad (101)$$

$$A_{0518} = h_g \Delta t \quad (102)$$

$$A_{0519} = h_f \Delta t \quad (103)$$

$$A_{0521} = -\frac{\Delta t}{V} \quad (104)$$

The first constitutive equation is mass fraction of non-condensable gases, which is the sixth row of matrix A_{vv}. Non-zero coefficient variables are convective quantity for non-condensable mass fraction (column 1), convective quantity for vapor density (column 2), and non-condensable mass fraction (column 6). Their off-diagonal coefficients can be obtained through Equations 105 and 106.

Coefficients in Mass Fraction of Non-condensable Gases Equation

$$A_{0601} = -\frac{1}{(\widehat{\alpha_g \rho_g})} \tag{105}$$

$$A_{0602} = \frac{(\widehat{\alpha_g \rho_g x_n})}{(\widehat{\alpha_g \rho_g})^2} \tag{106}$$

The second constitutive equation is vapor internal energy equation, which is the seventh row of matrix A_{vv}. Non-zero coefficient variables are vapor internal energy (column 7), convective quantity for vapor density (column 2), and convective quantity for vapor internal energy (column 4). Their off-diagonal coefficients can be obtained through Equations 107 and 108.

Coefficients in Vapor Internal Energy Equation

$$A_{0702} = -\frac{1}{(\widehat{\alpha_g \rho_g})} \tag{107}$$

$$A_{0704} = \frac{(\widehat{\alpha_g \rho_g u_g})}{(\widehat{\alpha_g \rho_g})^2} \tag{108}$$

The third constitutive equation is liquid internal energy equation, which is the eighth row of matrix A_{vv}. Non-zero coefficient variables are liquid internal energy (column 8), convective quantity for liquid density (column 3), and convective quantity for liquid internal energy (column 5). Their off-diagonal coefficients can be obtained through Equations 109 and 110.

Coefficients in Liquid Internal Energy Equation

$$A_{0803} = -\frac{1}{(\widehat{\alpha_f \rho_f})} \tag{109}$$

$$A_{0805} = \frac{(\widehat{\alpha_f \rho_f u_f})}{(\widehat{\alpha_f \rho_f})^2} \tag{110}$$

The fourth constitutive equation is vapor density equation, which is the ninth row of matrix A_{vv}. Non-zero coefficient variables are convective quantity for vapor density (column 9), non-condensable mass fraction (column 6), vapor internal energy (column 7), and total pressure (column 11). Their off-diagonal coefficients can be obtained through Equations 111-113.

Coefficients in Vapor Density Equation

$$A_{0906} = -\frac{\partial \rho_g}{\partial X_n} \tag{111}$$

$$A_{0907} = -\frac{\partial \rho_g}{\partial u_g} \tag{112}$$

$$A_{0911} = -\frac{\partial \rho_g}{\partial P} \tag{113}$$

Liquid density equation has two non-zero off-diagonal coefficient variables, which are liquid internal energy (column 8) and total pressure (column 11). Its coefficients are computed by Equations 114 and 115.

Coefficients in Liquid Density Equation

$$A_{1008} = -\frac{\partial \rho_f}{\partial u_f} \tag{114}$$

$$A_{1011} = -\frac{\partial \rho_f}{\partial P} \tag{115}$$

The sixth constitutive equation is void fraction equation, which is the eleventh row of matrix A_{vv}. Non-zero coefficient variables are convective quantity for vapor density (column 2), convective quantity for liquid density (column 3), vapor density (column 9), liquid density (column 10), and total pressure (column 11). Their off-diagonal coefficients can be obtained through Equations 116-119.

Coefficients in Void Fraction Equation

$$A_{1103} = \frac{1}{\rho_f} \tag{116}$$

$$A_{1110} = -\frac{(\widehat{\alpha_f \rho_f})}{\rho_f^2} \tag{117}$$

$$A_{1102} = -\frac{1}{\rho_g} \tag{118}$$

$$A_{1109} = \frac{(\widehat{\alpha_g \rho_g})}{\rho_g^2} \tag{119}$$

The seventh constitutive equation is vapor temperature equation, which is the twelfth row of matrix A_{vv}. Non-zero coefficient variables are vapor temperature (column 12), non-condensable mass fraction (column 6), vapor internal energy (column 7), and total pressure (column 11). Their off-diagonal coefficients can be obtained through Equations 120-122.

Coefficients in Vapor Temperature Equation

$$A_{1206} = -\frac{\partial T_g}{\partial X_n} \quad (120)$$

$$A_{1207} = -\frac{\partial T_g}{\partial u_g} \quad (121)$$

$$A_{1211} = -\frac{\partial T_g}{\partial P} \quad (122)$$

The thirteenth row contains liquid temperature equation, which has non-zero coefficient variables - liquid temperature (column 13), liquid internal energy (column 8), and total pressure (column 11). Their off-diagonal coefficients can be obtained through Equations 123 and 124.

Coefficients in Liquid Temperature Equation

$$A_{1308} = -\frac{\partial T_f}{\partial u_f} \quad (123)$$

$$A_{1311} = -\frac{\partial T_f}{\partial P} \quad (124)$$

The ninth constitutive equation is saturation temperature corresponding to partial pressure equation, which is the fourteenth row of matrix A_{vv}. Non-zero coefficient variables are saturation temperature corresponding to partial pressure of water vapor (column 14), non-condensable mass fraction (column 6), vapor internal energy (column 7), and total pressure (column 11). Their off-diagonal coefficients can be obtained through Equations 125-127.

Coefficients in Saturation Temperature Corresponding to Partial Pressure Equation

$$A_{1406} = -\frac{\partial T_{sp}}{\partial X_n} \quad (125)$$

$$A_{1407} = -\frac{\partial T_{sp}}{\partial u_g} \quad (126)$$

$$A_{1411} = -\frac{\partial T_{sp}}{\partial P_p} \quad (127)$$

Saturation temperature corresponding to total pressure equation has only one non-zero off-diagonal coefficient variable, which is total pressure. Its coefficient is computed by Equation 128.

Coefficients in Saturation Temperature Corresponding to Total Pressure Equation

$$A_{1511} = -\frac{\partial T_{sp}}{\partial P_p} \quad (128)$$

The eleventh constitutive equation is interface mass transfer equation, which is the sixteenth row of matrix A_{vv}. Non-zero coefficient variables are interface mass transfer (column 16), vapor temperature (column 12), liquid temperature (column 13), and saturation temperature corresponding to partial pressure of water vapor (column 14). Their off-diagonal coefficients can be obtained through Equations 129-131.

Coefficients in Interface Mass Transfer Equation

$$A_{1612} = -\frac{H_{ig}}{h_g^\circ - h_f^\circ} \quad (129)$$

$$A_{1613} = -\frac{H_{if}}{h_g^\circ - h_f^\circ} \quad (130)$$

$$A_{1614} = \frac{H_{ig}+H_{if}}{h_g^\circ - h_f^\circ} \quad (131)$$

The twelfth constitutive equation is interface energy exchange equation, which is the seventeenth row of matrix A_{vv}. Non-zero coefficient variables are interface energy transfer associated with interface mass transfer (column 17), vapor temperature (column 12), liquid temperature (column 13), and saturation temperature corresponding to partial pressure of water vapor (column 14). Their off-diagonal coefficients can be obtained through Equations 132-134.

Coefficients in Interface Energy Exchange Equation

$$A_{1712} = -\frac{h_f^\circ H_{ig}}{h_g^\circ - h_f^\circ} \quad (132)$$

$$A_{1713} = -\frac{h_g^\circ H_{if}}{h_g^\circ - h_f^\circ} \quad (133)$$

$$A_{1714} = -\frac{h_f^\circ H_{ig}+h_g^\circ H_{if}}{h_g^\circ - h_f^\circ} \quad (134)$$

Wall mass transfer to vapor equation is the eighteenth equation in A_{vv} matrix. Its non-zero coefficient variables are wall mall transfer to vapor (column 18), vapor temperature (column 12), liquid temperature (column 13), saturation temperature corresponding to partial pressure of water vapor (column 14), and saturation temperature corresponding to total

pressure (column 15). Their off-diagonal coefficients can be obtained through Equations 135-138.

Coefficients in Wall Mass Transfer to Vapor Equation

$$A_{1812} = -\frac{\Gamma_{wfg}}{\Delta t} \quad (135)$$

$$A_{1813} = -\frac{\Gamma_{wff}}{\Delta t} \quad (136)$$

$$A_{1814} = -\frac{\Gamma_{wfspp}}{\Delta t} \quad (137)$$

$$A_{1815} = -\frac{\Gamma_{wfspt}}{\Delta t} \quad (138)$$

Wall mass transfer to liquid equation is the nineteenth equation in A_{vv} matrix. Its non-zero coefficient variables are wall mall transfer to liquid (column 19), vapor temperature (column 12), liquid temperature (column 13), saturation temperature corresponding to partial pressure of water vapor (column 14), and saturation temperature corresponding to total pressure (column 15). Their off-diagonal coefficients can be obtained through Equations 139-142.

Coefficients in Wall Mass Transfer to Liquid Equation

$$A_{1912} = -\frac{\Gamma_{cgg}}{\Delta t} \quad (139)$$

$$A_{1913} = -\frac{\Gamma_{cgf}}{\Delta t} \quad (140)$$

$$A_{1914} = -\frac{\Gamma_{cgspp}}{\Delta t} \quad (141)$$

$$A_{1915} = -\frac{\Gamma_{cgspt}}{\Delta t} \quad (142)$$

The constitutive equation in twentieth row is wall heat transfer to vapor equation. Its non-zero coefficient variables are wall heat transfer to vapor (column 20), vapor temperature (column 12), liquid temperature (column 13), saturation temperature corresponding to partial pressure of water vapor (column 14), and saturation temperature corresponding to total pressure (column 15). Their off-diagonal coefficients can be obtained through Equations 143-146.

Coefficients in Wall Heat Transfer to Vapor Equation

$$A_{2012} = -\frac{Q_{wfg}V}{\Delta t} \quad (143)$$

$$A_{2013} = -\frac{Q_{wff}V}{\Delta t} \quad (144)$$

$$A_{2014} = -\frac{Q_{wfspp}V}{\Delta t} \quad (145)$$

$$A_{2015} = -\frac{Q_{wfspt}V}{\Delta t} \quad (146)$$

The last constitutive equation is wall heat transfer to liquid equation. Non-zero coefficient variables are wall heat transfer to liquid (column 21), vapor temperature (column 12), liquid temperature (column 13), saturation temperature corresponding to partial pressure of water vapor (column 14), and saturation temperature corresponding to total pressure (column 15). Their off-diagonal coefficients can be obtained through Equations 147-150.

Coefficients in Wall Heat Transfer to Liquid Equation

$$A_{2112} = -\frac{Q_{cgg}V}{\Delta t} \quad (147)$$

$$A_{2113} = -\frac{Q_{cgf}V}{\Delta t} \quad (148)$$

$$A_{2114} = -\frac{Q_{cgspp}V}{\Delta t} \quad (149)$$

$$A_{2115} = -\frac{Q_{cgspt}V}{\Delta t} \quad (150)$$

Another sub-matrix is constructed with the momentum conservation equation; therefor it is used to solve the increments in pressure, junction vapor velocity, and liquid velocity quantities in a 21 by 2 matrix called A_{jj}. Moreover, a complete matrix structure of a 4-volume pipe model is given as an example in Figure 4.

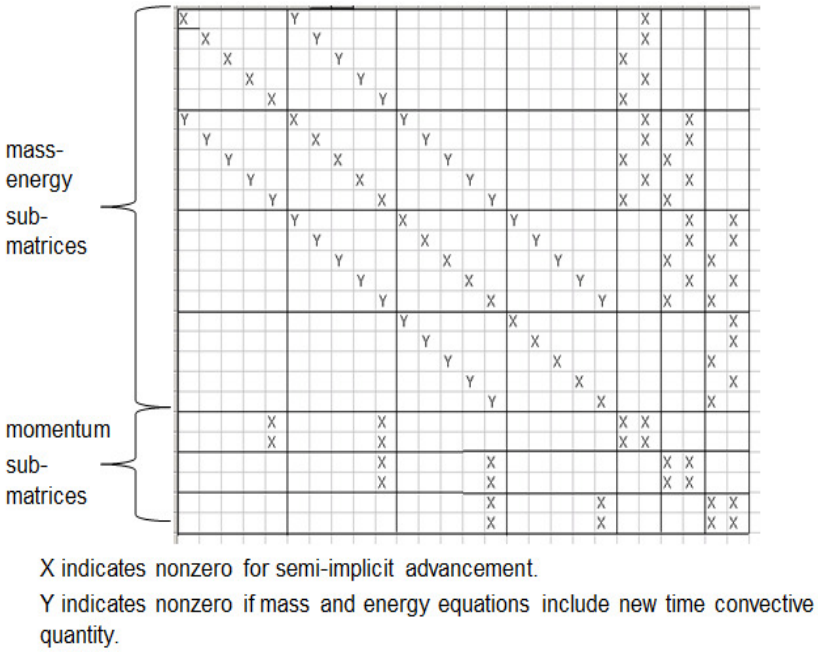

Figure 4: Matrix Structure of a 4-volume Pipe

Matrix A in Figure 4 is composed with both mass-energy and momentum sub-matrices. There are four columns of 5 by 5 matrices shown in Figure 2 and each one of them represents a 21 by 21 volume sub-matrix A_{vv} in Figure 1. Since a four-volume pipe has three inner junctions, there are six momentum equations for both phases. The momentum equations construct the bottom six rows in matrix A. These matrices representing liquid and vapor momentum equations have unknowns of changes in pressure and changes in velocity. The similar matrix A is built for each system. For example, a simplified one loop pressure water reactor contains two systems - primary loop and secondary loop, so it will construct and solve two matrices for each system at every time step.

The current conservative code solves a linear solution of conservation equations once every time step, so the convergent criterial was not studied in the scope of this paper. The future work will focus on solving the non-linear equations with Newton Raphson iteration. Therefore convergence will be studied in the future work related to the iteration. Moreover, several tests are performed to compare with the results from the original non-conservative approach. The comparisons are presented in the following sections.

Chapter 7: Test Results

In this section, six simple pipe models with different thermal hydraulic conditions and one simplified PWR steady state have been studied with RELAP5 in order to test the new solution strategy. The sample problems, which did show mass error reductions, were primarily designed to test code situations such as single phase flow of each phase, two phase flow, and transitions between single and two phase flow in each direction. The transitions are a difficult point in the simulation. The derivative terms in the approximation of the equations of state can change signs and orders of magnitude. The simulation relies on a time step control using halving and repeating of the time step to approach the transition point, using a very small time step to cross the transition, and then doubling back of the time step as permitted. The formulation of the two phase model limits void fractions to be within the values of 0 and 1, but the finite difference approximations to the conservation equations do not enforce those limits. Excessive violations cause time step reductions and repeat of time steps. Simply resetting the void fractions to the limits introduces mass error. Corrective action such as reducing the mass and energy interphase transfer rates are used to the extent possible. This handling of the transitions between single phase and two phase conditions is required in both the non-conservative and conservative form of the conservation equations. Test cases thus far have been focused on these situations. Table 1 briefly describes the test cases presented in the section.

Table 1 Testing Cases and Input Deck Description

Input Deck	Case Studies
cnsimpl.i	Case #1:signle phase liquid, equilibrium condition Case #2:two phase liquid and vapor in equilibrium condition Case #3:two phase liquid and vapor in non-equilibrium condition
cnsimplhs.i	Case #4:signle phase liquid with heat structure Case #5:two phase at equilibrium initial condition with heat structure Case #6:two phase at non-equilibrium initial condition with heat structure
splantstst.i	simplified PWR plant steady state

The first input deck is created based on a simple pipe model and the nodalization is shown in Figure 5. The system is horizontally orientated and it contains a one-volume pipe (Pipe_3), a trip valve (Valve_4), and a time dependent volume (TDV_5). The pipe has no heat structure attach to it, so there is no heat going in and out. Even though a trip valve is used, it is modeled as a closed valve through the simulation. Therefore, there is no mass transferring between the pipe and the outside world.

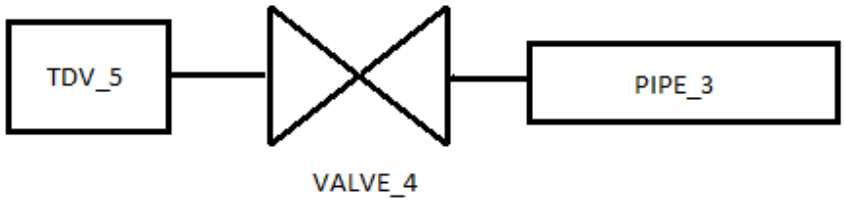

Figure 5 cnsimpl.i Nodalization

Table 2 presents geometry dimensions of all the components in the simple pipe model.

Table 2 Geometry Information In cnsimpl.i

TDV_5	L=0.204801m; Af=4.56037e-3m^2
Valve_4	Af=3.96752e-3m^2
Pipe_3	L=0.204801m; Af=4.56037e-3m^2; number of pipe volume: 1

There are three cases in the input deck cnsimpl.i and each one of them has a different initial condition within the pipe: Case#1 has a single phase liquid in pipe; Case#2 mimics two phases in an equilibrium condition; and Case#3 models two phases in non-equilibrium. The initial conditions are shown in table 3.

Table 3 Initial Conditions in cnsimpl.i

Initial Conditions	
TDV_5	P=1.0e5 Pa; Xs=1.0
Valve_4	Closed through the entire problem
Pipe_3 in Case#1	P=7.0e6Pa; Uf=9.78293e5J/kg; Ug=2.58184e6J/kg; voidg=0.0(equilibrium)
Pipe_3 in Case#2	P=7.0e6Pa; Xs=0.5 (equilibrium)
Pipe_3 in Case#3	P=7.0e6Pa; Uf=1.27e6J/kg; Ug=2.6e6J/kg; voidg=0.5(non-equilibrium)

Case#1 models a single phase liquid in a one-volume pipe, which is completely isolated from the outside environment. Consequently, the fluid properties are constant. Figures 6 to 8 represent comparisons of pipe pressure, liquid temperature, and liquid internal energy in Case#1 between the conservative and the non-conservative forms of simulation results.

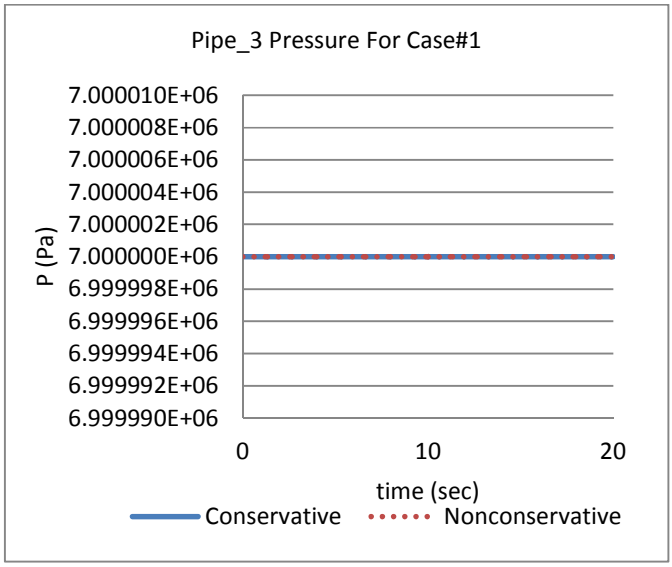

Figure 6 Case#1 Pressure Comparison

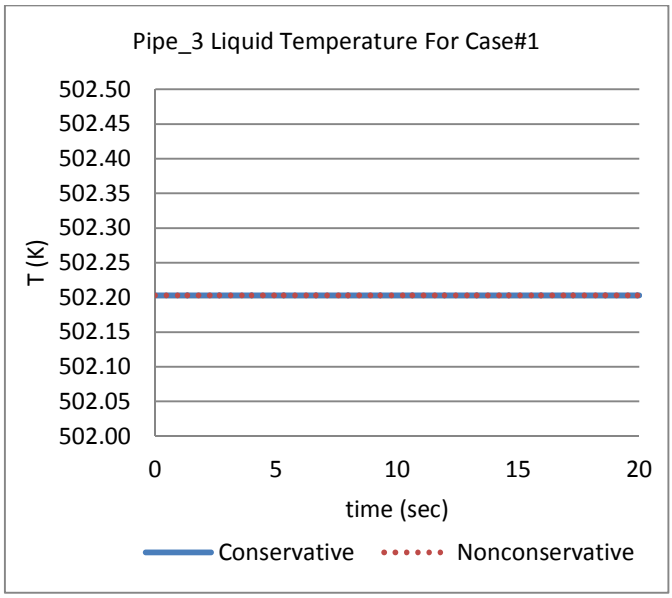

Figure 7 Case#1 Liquid Temperature Comparison

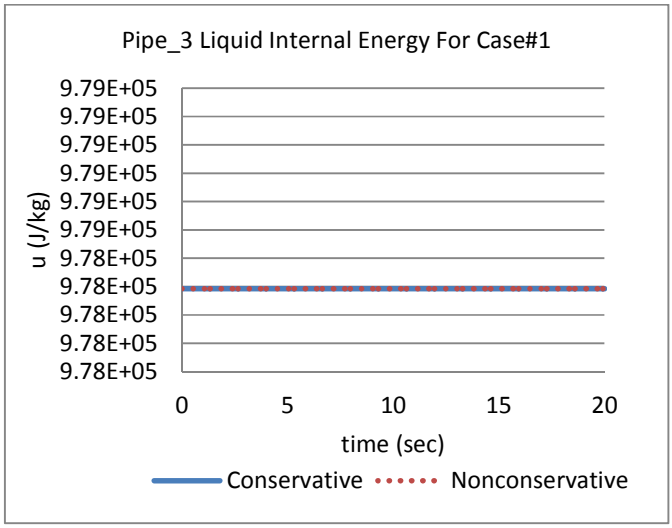

Figure 8 Case#1 Liquid Internal Energy Comparison

The percent differences of pressure, liquid temperature, and liquid internal energy between the conservative and non-conservative results are zeros. It means, in the Case#1 simple pipe model, the conservative form gives the exactly same results as the non-conservative form does.

The second test in the same input deck is more interesting since there are both liquid and vapor presenting in the pipe. Figure 9 and Figure10 show the vapor void fraction and the vapor internal energy values.

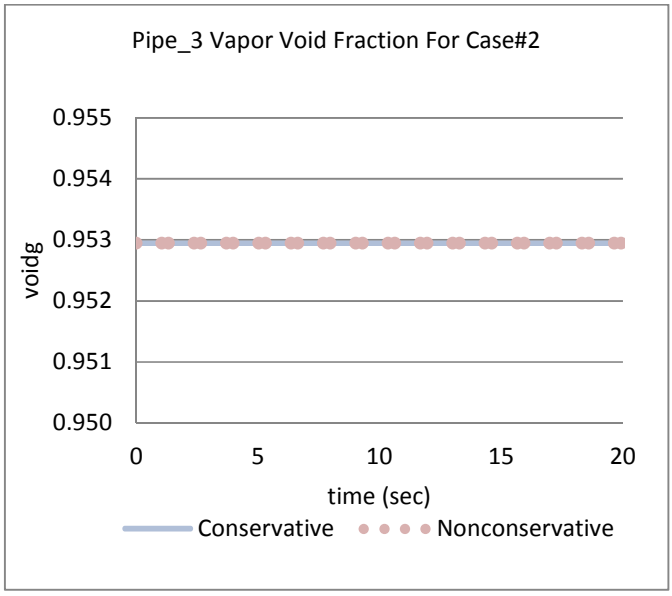

Figure 9 Case#2 Vapor Void Fraction Comparison

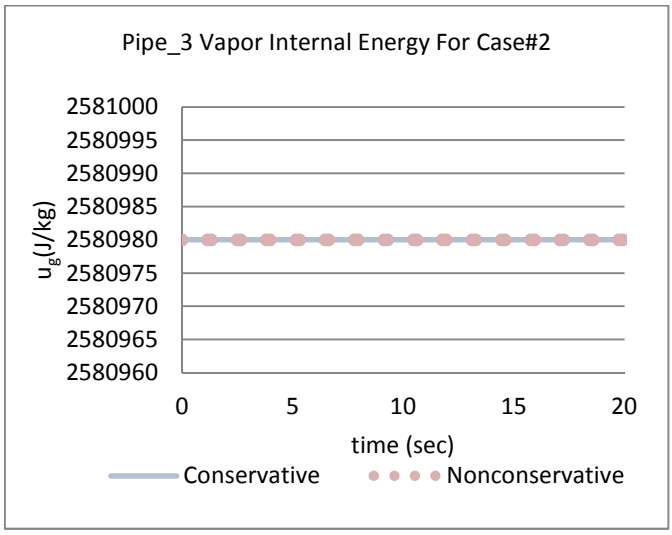

Figure 10 Case#2 Vapor Internal Energy Comparison

The results from the conservative from match exactly the non-conservative form, so the computed percent difference is zero. In Case#2, vapor void fraction does not change due to the fact that liquid and vapor coexist at the equilibrium condition. Moreover, the non-

equilibrium condition is tested by the last case in cnsimpl.i. Therefore, interphase mass/energy transfers occur.

Figure 11 and 12 show the comparisons of vapor void fraction and the vapor generation rate in Case#3.

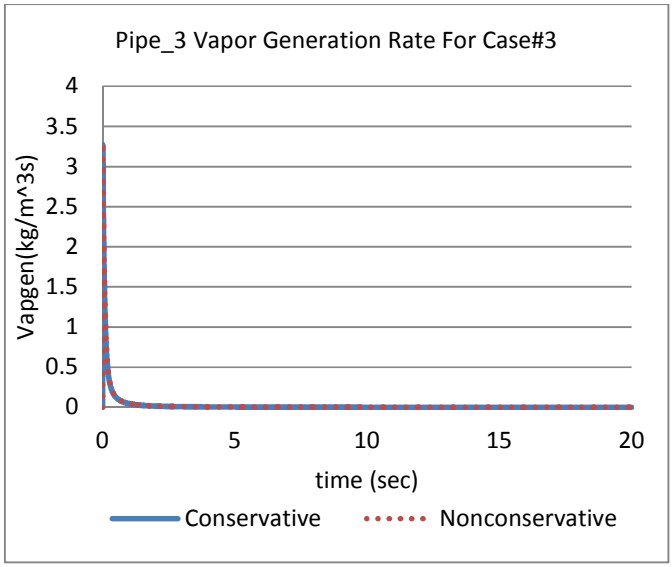

Figure 11 Case#3 Vapor Generation Rate Comparison

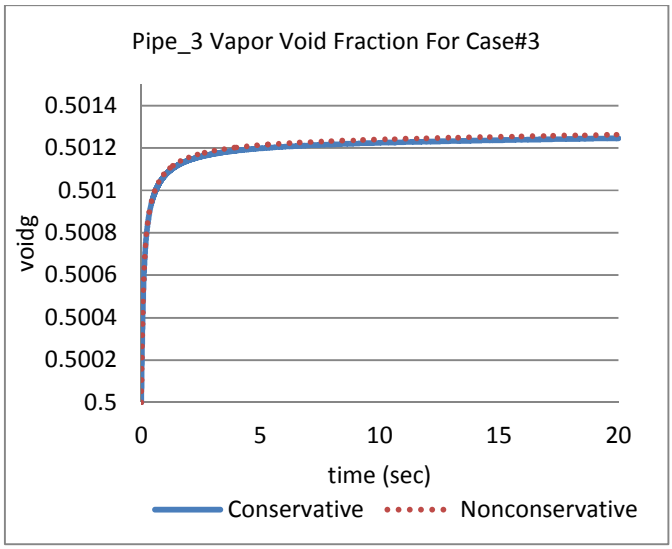

Figure 12 Case#3 Vapor Void Fraction Comparison

It may appear that discrepancy is more noticeable in the vapor void plot of Case#3. However, the percent differences in the conservative and non-conservative forms are very small. At 20 seconds of the run time, it is about 0.003% difference.

'emass' is one of the general quantities in RELAP5. It is computed within the code and used to estimate of mass errors in all systems. Finally, the absolute values of mass errors in the conservative and non-conservative forms are compared and presented in Figure 13. As appeared in the plot, the conservative form gives much smaller mass error values than the non-conservative form does. At the end of the run, the conservative form results a mass error in an order of ten to the negative ten comparing to .00014 from the non-conservative approach.

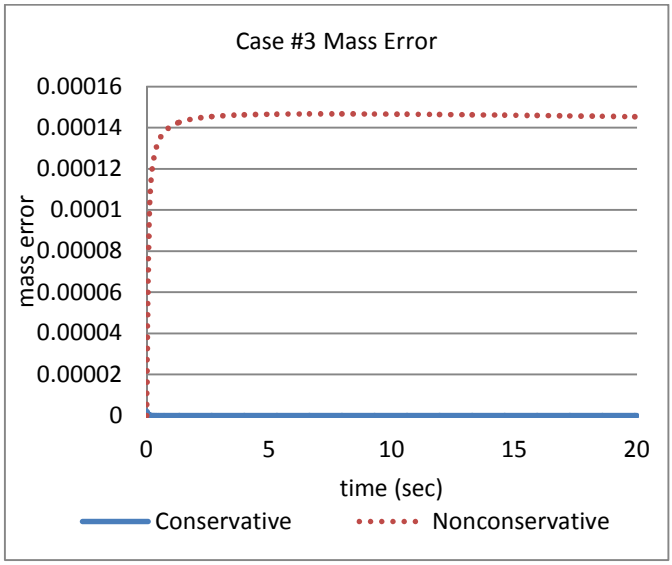

Figure 13 Case#3 Mass Errors

Even though mass errors exist in these simple pipe models, magnitudes of the errors are small and have no effect on simulation results. Therefore, the results from the non-

conservative code can be used to verify the improved code. The comparison tests show that the conservative code predicts the same thermal hydraulic behavior as the non-conservative does. Meanwhile, mass error comparison plots show that a better accuracy or less mass error can be achieved with the fully conservative approach.

The second input deck is an extension of cnsimpl.i. The system shown in Figure 14 is the same as the previous model. It has a one-volume pipe (Pipe_3), a trip valve (Valve_4), and a time dependent volume (TDV_5). The pipe has a heat structure (Hts_3) attach to it. The heat structure mimics a wall of the pipe and has no power within it. C-steel is used as the heat structure material. Even though a trip valve is used to connect the time dependent volume and the pipe, it is modeled as a closed valve through the simulation and there is no mass transfer into or out of pipe. Nodalization is shown below:

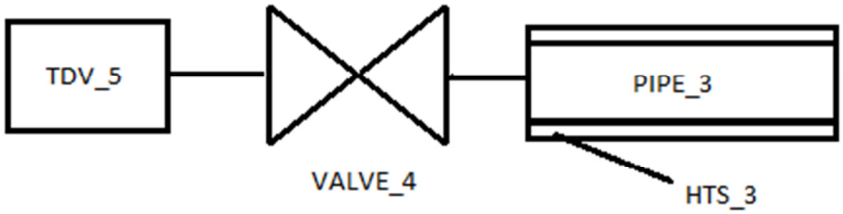

Figure 14 cnsimplhs.i Nodalization

Table 4 presents geometry dimensions of all the components in the model.

Table 4 Geometry Information in cnsimplhs.i

TDV_5	L=0.204801m; Af=4.56037e-3m^2
Valve_4	Af=3.96752e-3m^2
Pipe_3	L=0.204801m; Af=4.56037e-3m^2; number of pipe volume: 1
Hts_3	Thickness=0.0381m; Heated length=0.204801m

Testing cases 4 to 6 are in the input deck and each has a different initial condition within the pipe: In Case#4, pipe has a single phase liquid; Case#5 mimics two phase in equilibrium condition; and Case#6 models two phases in non-equilibrium. The initial conditions are shown in table 5. Unlike cnsimpl.i model, cnsimplhs.i has heat transfer through the heat structure.

Table 5 Initial Conditions in cnsimplhs.i

Initial Conditions	
TDV_5	P=1.0e5 Pa; Xs=1.0
Valve_4	Closed through the entire problem
Pipe_3 in Case#4	P=7.0e6Pa; Uf=9.78293e5J/kg; Ug=2.58184e6J/kg; voidg=0.0(equilibrium)
Pipe_3 in Case#5	P=7.0e6Pa; Xs=0.5(equilibrium)
Pipe_3 in Case#6	P=7.0e6Pa; Uf=1.27e6J/kg; Ug=2.6e6J/kg; voidg=0.5(non-equilibrium)
Hts_3	No heat source; Isolated right boundary; $T_{initial}$=600K

Cnsimplhs.i is the same as cnsimpl.i besides the pipe wall is modeled with heat structure; therefore the comparison test mainly focuses on the newly introduced the heat structure related parameters, such as heat fluxes (RELAP5 parameter-HTRNR), heat structure average temperatures (RELAP5 parameter-HTVAT), and interface mass transfers due to wall boundary conditions (RELAP5 parameter-GAMMAW).

Since all three cases are very similar, the results of Case#4 alone are analyzed to represent the group of simulations in cnsimplhs.i. Case#4 initially has liquid in the pipe at an equilibrium condition. Then a small amount of vapor is generated due to the heat addition from the heat structure to the pipe. At the end, simulation reaches a steady state and vapors

condense. Figure 15 and 16 show the comparisons of the heat structure parameters, including the heat fluxes between pipe/wall and the volume-average heat structure temperature, resulted from the conservative form and the non-conservative form. The outside of wall (left boundary of heat structure) is isolated, so heat flux is zero and only heat flux at inner wall (right boundary of heat structure) is plotted here.

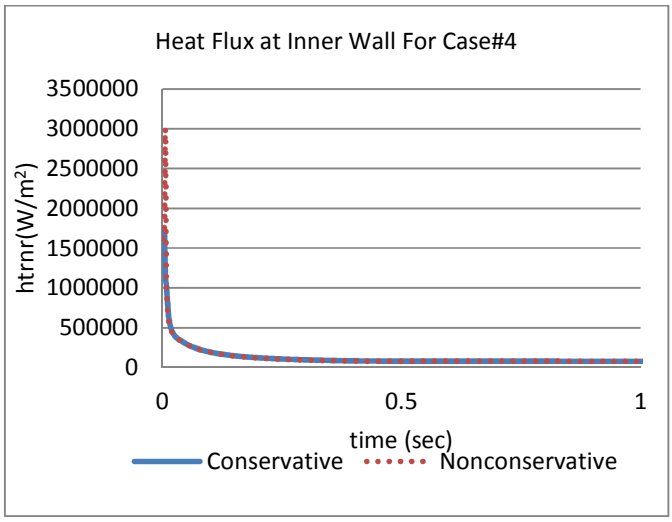

Figure 15 Case#4 Heat Flux at Inner Wall Comparison

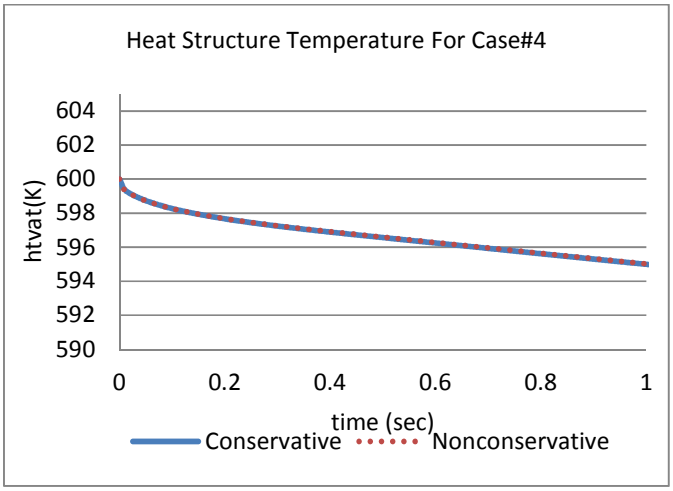

Figure 16 Case#4 Heat Structure Temperature Comparison

The heat structure temperatures of Case#4 are compared and the percent differences are presented in Figure 17. Finally, the mass error resulted from the simulation is compared. At the end of the time step, the total mass error from the conservative approximation approach gives about 1.147E-7. The non-conservative form results a mass error at around 1.7E-5, which is about 100 times larger.

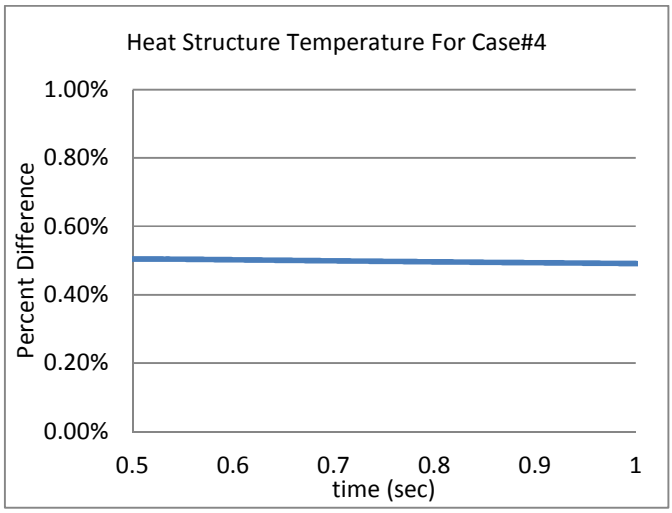

Figure 17 Case#4 Heat Structure Temperature Percent Difference

The fully conservative numerical approximation in RELAP5 is also tested with a simplified pressure water reactor plant simulation. The input deck splantstst.i is used to achieve a steady state condition during the PWR normal operation. The plant nodalization is shown in Figure 18.

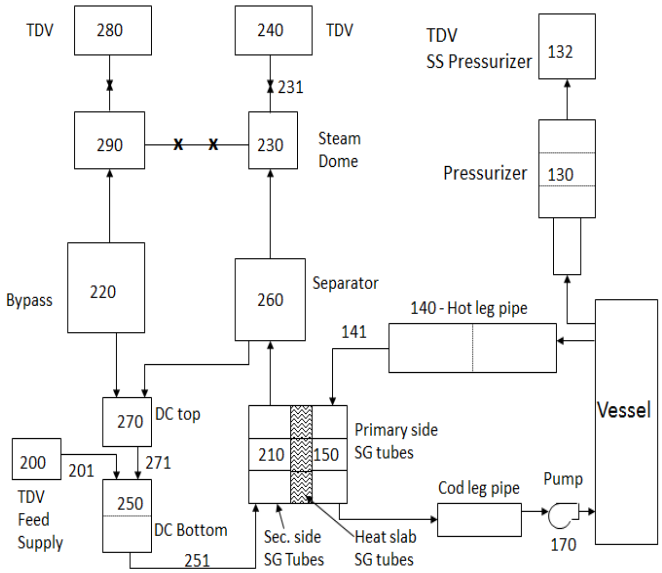

Figure 18 Simplified PWR Nodalization

The primary system contains system pipings, a core vessel containing the nuclear core, a pressurizer with a surge line, a steam generator, and a Westinghouse pump. The secondary loop includes a steam generator tube sheet, a separator, a steam dome, a steam dome outlet time dependent volume, and a downcomer annulus with a feedwater inlet. The heat slab of the steam generator tubes is modeled with the heat structure 150 (Hst_150) with 3 heat structure volumes, which are shaded areas in Figure 18. Table 6 gives the initial condition values.

Table 6 Initial Conditions in splantstst.i

Primary system	pressure	15 MPa
	loop average temperature	550 K
	loop flow rate	131 kg/sec
	core power	50 MW
Secondary System	pressure	2 MPa
	feedwater flow rate	26.1 kg/s
	feedwater temperature	478 K

The primary pressures in volume_140 [Fig 18] of the conservative form and the non-conservative form are compared and presented in Figure 19. The percent differences in pressures are plotted in Figure 20. The differences disappear once the simulations archive steady state.

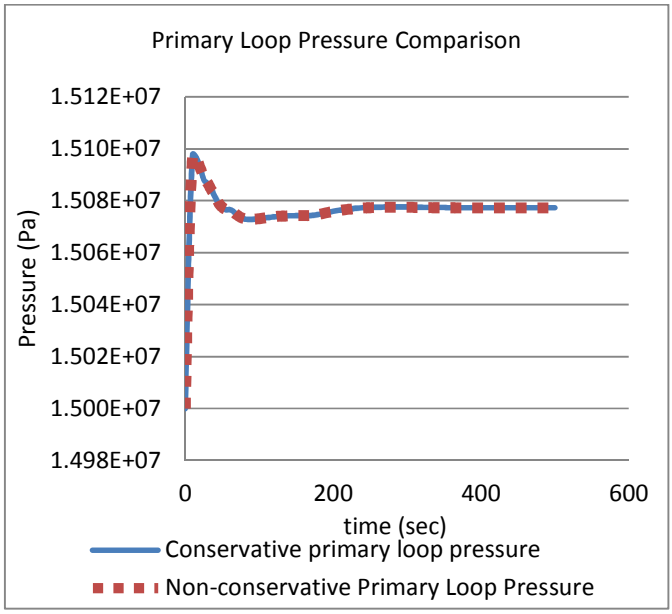

Figure 19 Simplified PWR Primary Loop Pressure Comparison

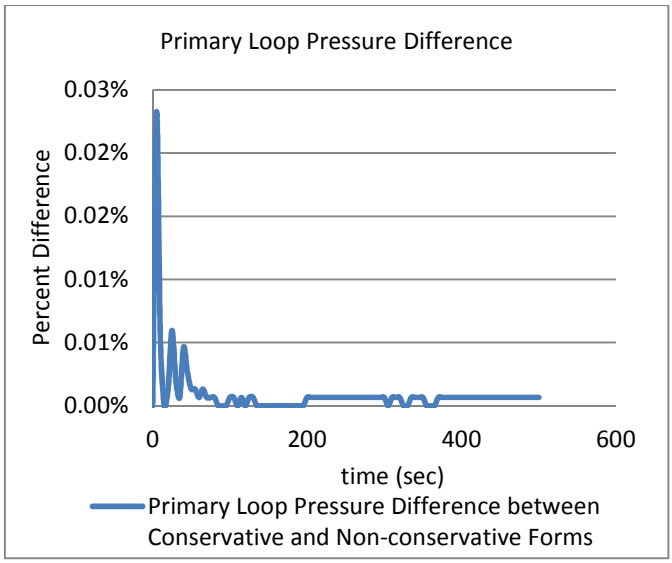

Figure 20 Simplified PWR Primary Loop Pressure Difference

The temperature of the steam generator separator is the second parameter to be compared. Figure 21 plots the temperature values of the steady state condition and the

percent differences are computed and plotted in Figure 22. During steady state, the conservative and non-conservative numerical approaches produce the same results.

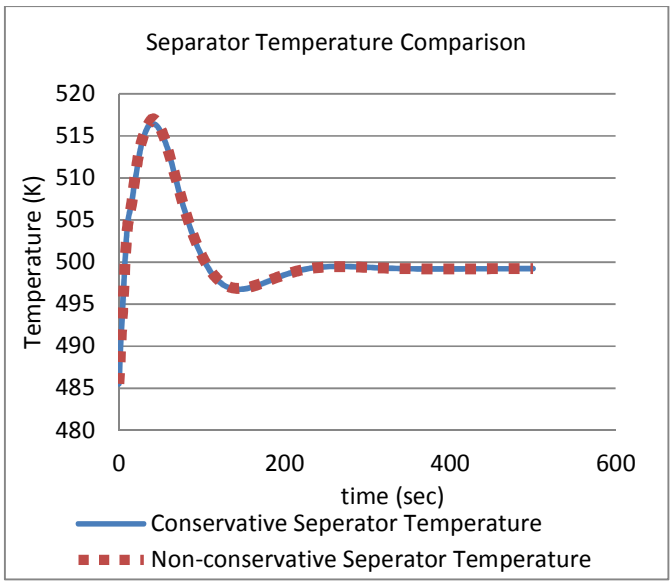

Figure 21 Simplified PWR Separator Temperature Comparison

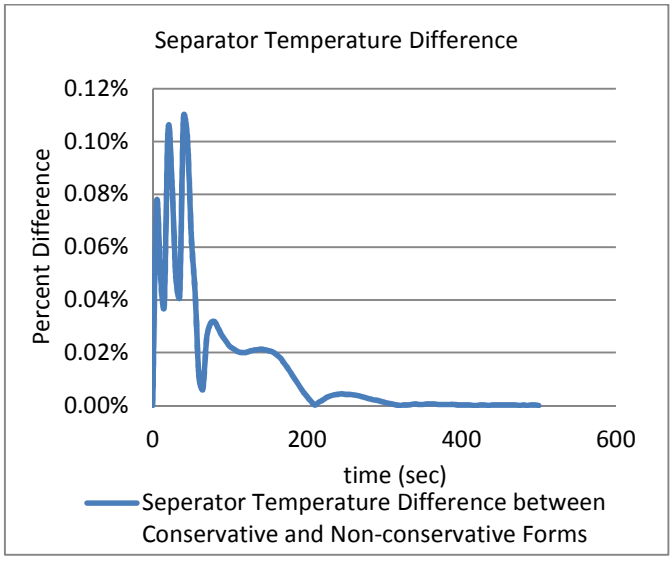

Figure 22 Simplified PWR Separator Temperature Difference

Another volume parameter - vapor void fraction in separator is compared in Figure 23 and the percent differences between the conservative method and the non-conservative method are present in Figure 24.

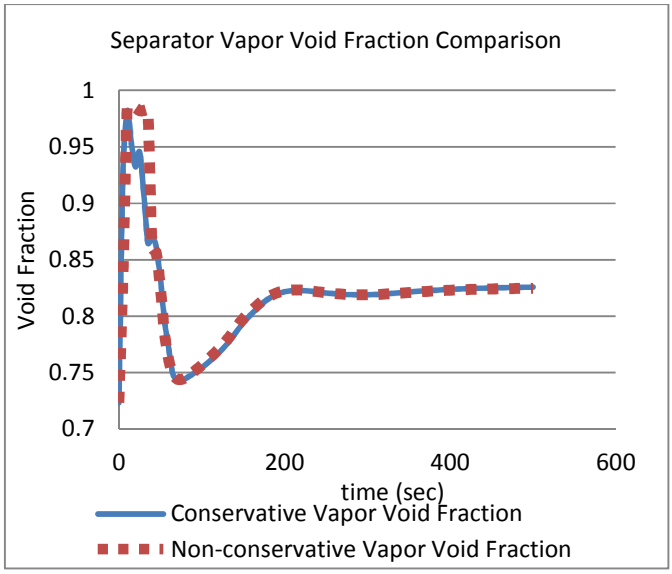

Figure 23 Simplified PWR Separator Vapor Void Fraction Comparison

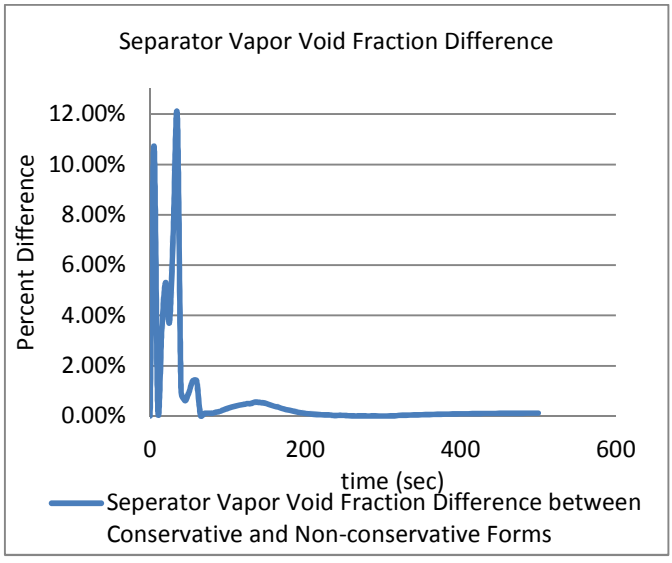

Figure 24 Simplified PWR Separator Vapor Void Fraction Difference

Next, one junction parameter (junction velocity) and one heat structure parameter (heat flux values) are shown in Figure 25 and Figure 26 separately. Heat structure volume 1502 is the center volume of the steam generator; and the junction velocities are ones in the steam generator inlet junction 141 [Fig 18].

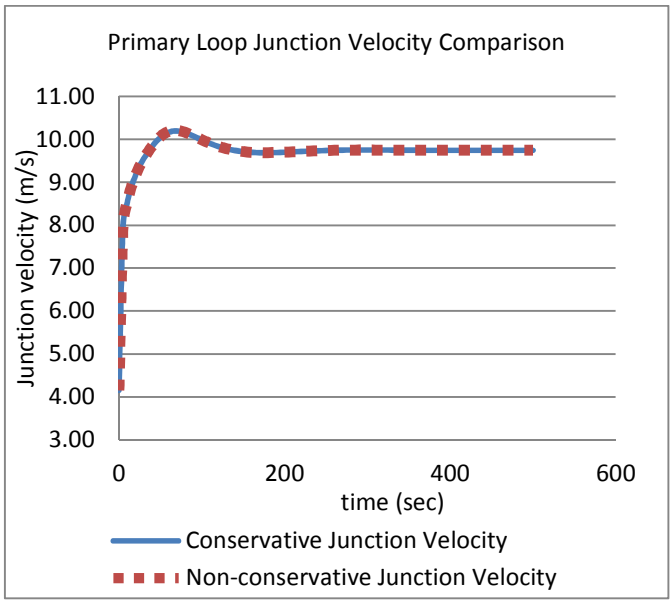

Figure 25 Simplified PWR Primary Loop Junction Velocity Comparison

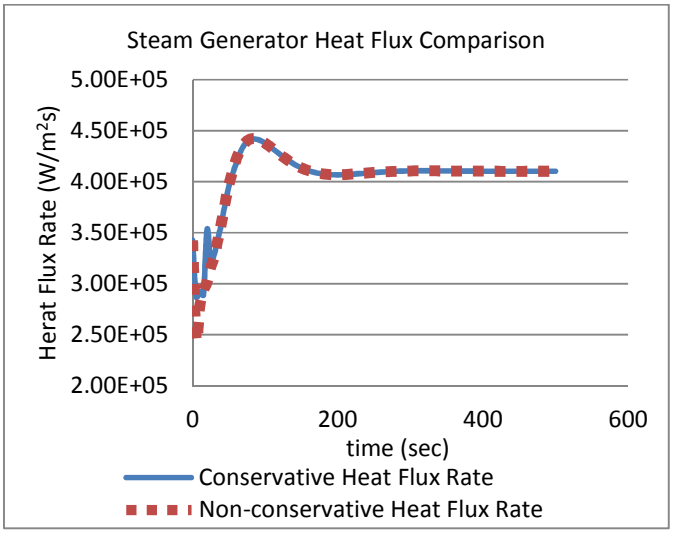

Figure 26 Simplified PWR Steam Generator Heat Flux Comparison

The results give percent differences in ~0.001% for heat flux and ~0.002% for junction velocity at steady state condition. The purpose of this simplified PWR plant comparison is to show that the new conservative code is able to simulate a complete plant model and the predictions are similar to the non-conservative numerical approximation.

However, the main motivation of the work is to reduce mass error by implementing a fully conservative form. Therefore, the mass error comparison between the conservative and non-conservative forms is plotted in Figure 27.

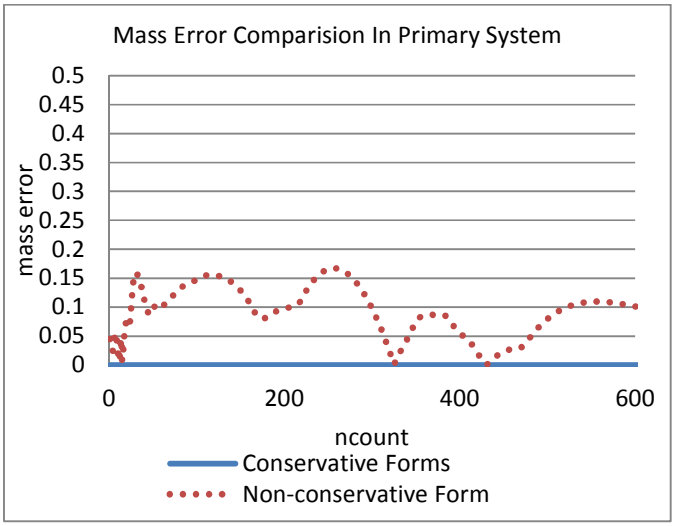

Figure 27 Simplified PWR Primary System Mass Error Comparison

Since the mass error from the conservative form is extremely small, Figure 27 is not able to present the value of conservative mass error. Therefore, a zoomed plot for the conservative mass error is re-plotted in Figure 28.

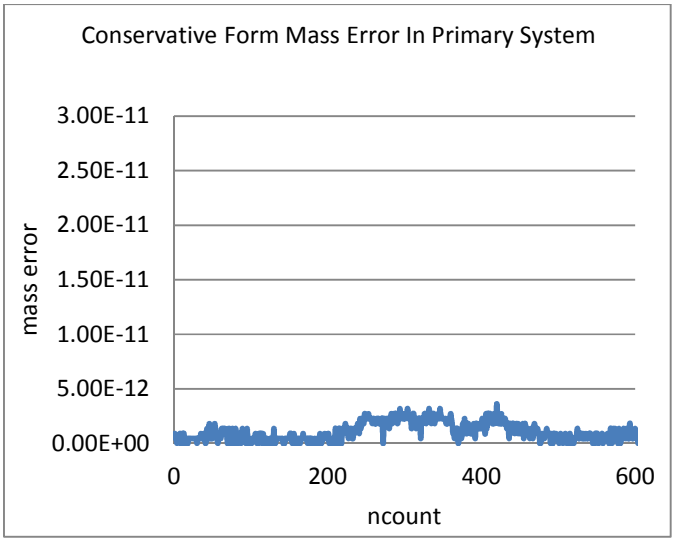

Figure 28 Simplified PWR primary system mass error conservative forms

The simple plant mass error comparison shows that a large amount of mass error reduction is achieved in a fully conservative code.

The significant benefit of the fully conservative approach is also demonstrated by Table 7. Table presents some of testing models and lists them in the ascending complexity order. Complexity is ranked by number of components and thermal hydraulic conditions in the models. For example, models with flow or heat structure are more complex than ones without flow or heat structure and non-equilibrium model is more complex than equilibrium condition. As shown in Table 7, conservative code is able to reduce mass error by about factor of 10^{12} in all testing cases.

The table also shows that PWR plant model, which has much more components than simple pipe does, results about 1000 times bigger mass error. When models become more complex, mass errors increase. Therefore, as models becoming more complex, they can be troublesome for non-conservative code by continually increasing mass error. Eventually, large errors will lead to incorrect simulation results in non-conservative code. However, expectation from conservative code is that it will reduce the mass error by factor of 10^{11} and keep them at low values even in more complex simulations, so the correct simulation results can be obtained.

Table 7 Mass Error Comparison Table

	Test Cases	Mass error (non-conservative form)	Mass error (conservative form)	Ratio of conservative to non-conservative
1	Pump test	8.830810E-04	3.13296E-14	3.547761E-11
2	Simple pipe with power input, no flow	1.639210E-03	3.191890E-16	1.947212E-13
3	Simple pipe with flow and power	0.0354538	1.065210E-12	3.004502E-11
4	PWR Plant	0.1042274	3.1832310E-12	3.054121E-11

Chapter 8: Conclusion

The desirability of the more conservative form of the conservation equations is due to the mass and energy within the bounds of the problem being conserved over time advancements. Thus, even though truncation error may not allow the mass and energy to be properly distributed over the volume of the problem, the total mass and energy within the system are preserved. A method that preserves that total mass and energy is intuitively more attractive than one that does not conserve total mass.

In the RELAP5 semi-implicit method, a non-conservative form of the conservation equations is used. The solution values are consistent in that the solution can be checked by substituting the new time values into the simultaneous equations resulting from the numerical approximation to the hydrodynamic equations. Then, the conservation equations of mass and energy are rewritten using the more conservative form of those equations and using results from the prior non-conservative solution as needed. The equations can be explicitly solved (no simultaneous equations) for the convective quantities, vapor void fraction times vapor density times non-condensable mass fraction and the void fraction times density and void fraction time density times internal energy for each phase. New internal energies are obtained by dividing the product of the void fraction, density, and internal energy by the void fraction times density for each phase. New void fractions can be obtained by dividing the product of the void fraction, and densities by the extrapolated densities for each density obtained during the first step. But if that is done, the void fractions do not necessarily sum to 1.0. So instead, the two phases are mixed and the void fraction is determined from the mixture equation. This step seems to introduce mass errors and may negate gains made from using the conservative form of the mass and energy equations in the second step. The proposed change to the

solution of the conservation equations offers a conservative form of the conservation equations in a consistent, single step method.

Even though the current conservative code increases computational effort, the computing time of using the new solution strategy heavily depends on the ability and efficiency of the sparse matrix solver used. The current code uses MA28 sparse matrix solver. Switching to the most recent sparse matrix solver, such as Intel Math Kernel Library, could improve the efficiency and reduce the simulation run time.

There are other possible means of increasing speed of the conservative form. Simple replacement operations can be used to eliminate variables and equations from the complete set of equations for each volume. Four of the equations for each volume define four different temperature changes as functions of pressure and internal energy using a two term Taylor series approximation of the equation of state. Six other equations use the four temperature changes to define mass and energy transfers between the phases and heat transfer between the vapor and liquid and heat structures. The equations defining the temperature changes from the equation of state are used to replace the temperature changes in the six equations. The effect is that the four equations defining the temperature changes can be set aside for later use in back substitution, and four equations per volume have been removed from the set of simultaneous equations. The six equations define six quantities appearing in the conservation of mass and energy equations. Similarly, these quantities can be replaced in the mass and energy equations, allowing six more equations to be set aside. This is continued for additional equations until only six equations per volume remain the set of simultaneous equations for the conservative form and five equations remain for the non-conservative form. This simple replacement is possible because a replacement could be done using only one

equation to define a replacement. If more equations are required to define replacements, the operation is more difficult. The replacement operations were originally performed manually. But since that task is tedious and errors are easily introduced, Mathematica was used to do the replacements.

The instability relates to the fundamental finite difference methods used in the codes (semi-implicit for this study); in addition, another cause is the explicit time evolution of friction and heat transfer terms (Mahaffy, 1993). The stability of semi-implicit method has been studied (Liles, D. R., Reed, WM. H., 1978). The new conservative code does not change the semi-implicit scheme, nor does it alter the way of evaluating friction and heat transfer terms. Therefore, it is believed that the more conservative form does not introduce new sources of instability. Moreover, as part of this work, it is intended to test small change to allow Crank-Nicolson advancement. An explicit advancement using only old time values for space oriented quantities would not require solution of simultaneous equations, but time steps would be severely limited by stability considerations to a sonic velocity based limit. Using new time values for the space oriented quantities requires the solution of simultaneous equations but larger time steps can be used. The semi-implicit advancement used new time values for only selected quantities such that time steps up to a material transport limit are possible and the simultaneous equations could be readily solved. Later, a nearly-implicit method which used additional new time information was added which removed the stability limit but required more run time per advancement in order to handle the larger set of simultaneous equations. Moving to Crank-Nicolson advancement is simply the replacing the use of a new time value with the average of the new and old time values. Intuitively, this seems desirable since given a purely integration problem, one would select a trapezoidal

based numerical integration over a rectangle based integration. Advancements using Crank-Nicolson can generate oscillatory behavior even though the advancement is unconditionally stable. The heat conduction advancement in RELAP5 uses Crank-Nicolson advancement. Tests of the heat conduction advancement procedures were run comparing Crank-Nicolson and fully implicit advancement at varying time steps for problems having analytical solutions. Oscillatory behavior for the Crank-Nicolson was observed, but it was also noted that the fully implicit advancement was highly damped. An average of the oscillatory behavior may have been nearer to the analytical solution than the fully implicit advancement. Use of the Crank-Nicolson technique may require improved time step control.

Simple models (with a wide range of thermal-hydraulic conditions) are built for testing the new code and six simple pipe cases are presented in paper to show comparable results from conservative form. The tests focus on volume, junction, and heat structure parameters. In future work, other RELAP5 parameters like trip variables and control variables will be tested. A more complicated PWR plant is also tested for code accuracy and ability to simulate a complete plant model.

The mass error comparison tests show that improved code is able to reduce mass error by a factor of about 10^{11}. Moreover, mass error increases with more complex models. As complexity goes up, models can become troublesome for non-conservative code because of continually increased mass errors. Eventually, large errors will lead to incorrect simulation results. However, conservative code will reduce the mass error by factor of 10^{11} and avoid to result a large mass error, so the correct simulation results can be preserved by the improve code.

The work of implementing fully conservative forms into RELAP5 is a continuing task. The status quo of the study is presented in this part II of the series paper. The main purpose is to introduce an innovative strategy for implementing and solving fully conservative mass and energy equations. The small differences between two codes are targeted because the new version of RELAP5 is supposed to predict the same results with smaller mass error (the main motivation of the work). Moreover, the comparison tests results prove that the solution strategy is feasible and a mass error reduction by using conservative forms is observed. The future wok will focus on implementing iteration method to improve the accuracy, improving code robustness with Crank-Nicolson scheme, and improving efficiency of the fully conservative forms.

References

1. NSAD (Nuclear Safety Analysis Division), 2001. RELAP5 Code Manual Volume I Code Structure, System Models, and Solution Methods. Information System Laboratories, NUREG/CR-5535/Rev 1-Vol I.

2. Ransom, V.H., 1989. Course A-Numerical Modeling of Two-Phase Flows for Presentation at Ecole d'Ete d'Analyse Numerique. EGG-EAST-8546, Idaho National Engineering Laboratory.

3. Roth, G. A., Aydogan, F., 2014a. Theory and Implementation of Nuclear Safety System Codes – Part I: Conservation Equations, Flow Regimes, Numerics and Significant Assumptions, 76, 160-182.

4. Roth, G. A., Aydogan, F., 2014b. Theory and Implementation of Nuclear Safety System Codes – Part II: System Code Closure Relations, Validation, and Limitations, 76, 55-72.

5. (USNRC, TRACE V5.0), United States Nuclear Regulatory Commission, Field Equations, Solution Methods, and Physical Models. TRACE V5.0 Theory Manual.

6. Mahaffy, J. H., Numerics of codes: stability, diffusion, and convergence, Nuclear Engineering and Design, 131-145

7. Rg. 1.203, Regulatory Guide 1203, U.S.-NRC, December, 2005

8. Liles D. R., Reed, WM. H., 1978, A Semi-implicit Method for Two-Phase Fluid Dynamics, Journal of Computational Physics 26, 390-407